Quaternary Science Reviews 345 (2024) 109045

Contents lists available at ScienceDirect

Quaternary Science Reviews

journal homepage: www.elsevier.com/locate/quascirev

Holocene summer temperature reconstruction from plant *sed*aDNA and chironomids from the northern boreal forest

Roseanna J. Mayfield [a,b,c,*], Dilli P. Rijal [d], Peter D. Heintzman [d,e,f], Peter G. Langdon [a], Dirk N. Karger [g], Antony G. Brown [a,d], Inger G. Alsos [d]

[a] School of Geography and Environmental Science, University of Southampton, Southampton, SO17 1BJ, UK
[b] School of Geography Politics and Sociology, Newcastle University, Newcastle-upon-Tyne, NE1 7RU, UK
[c] Division of Agricultural and Environmental Sciences, School of Biosciences, Sutton Bonington Campus, University of Nottingham, Sutton Bonington, Loughborough, Leicestershire, LE12 5RD, UK
[d] The Arctic University Museum of Norway, UiT - the Arctic University of Norway, Tromsø, Norway
[e] Centre for Palaeogenetics, Svante Arrhenius väg 20C, Stockholm, SE-10691, Sweden
[f] Department of Geological Sciences, Stockholm University, Stockholm, SE-10691, Sweden
[g] Swiss Federal Institute for Forest, Snow and Landscape Research WSL, Switzerland

ARTICLE INFO

Handling editor: P Rioual

Keywords:
*sed*aDNA
Chironomids
Holocene
Palaeolimnology
Boreal
Temperature reconstructions
Trait-based reconstruction

ABSTRACT

Climate-induced ecotonal shifts are expected to occur in the (sub)arctic and boreal zones in the coming decades. Understanding how these ecosystems have previously responded to climate change can provide greater insight into how ecosystems may develop under existing and future pressures. Here we present a Holocene record from Lake Horntjernet, a lake on the northern edge of the boreal forest in Northern Norway. We show vegetation development and landscape dynamics typical for Northern Fennoscandia during the Holocene. A plant *sed*aDNA record indicates rapid vegetation development following deglaciation with early arrival of *Betula* trees/shrubs. Pine forest was established by c. 8500 cal yr BP, and subsequent mid- to late Holocene vegetation assemblages are relatively stable. The aquatic ecosystem community is indicative of climatic change during the early Holocene, while strong coupling with changes in the catchment vegetation affects the water quality during the mid- and late Holocene. The chironomid record indicates lake water acidification following the establishment of pine forest and heathland. Different approaches for temperature reconstruction are calculated and the results are compared to better understand ecosystem-climate relationships and ecosystem resilience to climate change. Chironomid-inferred temperatures indicate early Holocene warming and late Holocene cooling, comparable to independent regional temperature trends. However, lake acidification impedes reliable reconstruction of chironomid-inferred temperatures in the mid-Holocene, a trend recognised in other boreal chironomid records. The application of *sed*aDNA plant-inferred summer temperature reconstruction is inhibited by the persistence of cold and warm tolerant species within the boreal pine forest. However, a trait-based approach reconstructed temperature trends that aligned with independent regional data. Thus, here we demonstrate the value of combined molecular and fossil-based proxies for elucidating the complex response of a boreal catchment to climate change.

1. Introduction

The world is warming at an unprecedented rate (Post et al., 2019; Smith et al., 2015), with the Arctic warming twice as fast as the global average (IPCC et al., 2018; Walsh et al., 2016). These changes in climate have driven recent wide-scale changes in the composition, density, and distribution of Arctic vegetation (Elmendorf et al., 2012; Macias-Fauria et al., 2012). Such vegetation shifts are likely to continue under current climate predictions, with woody vegetation cover increasing by potentially 52% across the Arctic by 2050 CE (Pearson et al., 2013). Changes in the terrestrial vegetation in lake watersheds can strongly influence lake water state, thus affecting lake ecosystems (Cardille et al., 2007; McGowan et al., 2018), yet knowledge of terrestrial-aquatic relationships in high-latitude, treeline-tundra environments is limited

* Corresponding author. School of Biosciences, University of Nottingham, Sutton Bonington Campus, Sutton Bonington, Leicestershire, LE12 5RD, UK.
E-mail address: roseanna.mayfield@nottingham.ac.uk (R.J. Mayfield).

https://doi.org/10.1016/j.quascirev.2024.109045
Received 5 June 2024; Received in revised form 24 October 2024; Accepted 25 October 2024
Available online 30 October 2024

(McGowan et al., 2018). Lakes situated at ecotonal boundaries are of particular interest for climate reconstructions as small changes in climatic or environmental conditions can cause large biotic changes (Körner, 1998; MacDonald et al., 1993). Multiproxy palaeoecological archives provide insight into changes in both edaphic and biotic factors under changing climates and environments, and therefore offer a more comprehensive understanding of localised climate dynamics (Birks and Birks, 2006). Here, we combine proxies representing changes in landscape dynamics and lake development to investigate the utility of biotic proxies to reconstruct temperature at the northern limit of the boreal ecotone.

Terrestrial ecosystems are highly sensitive to changing climates (Nolan et al., 2018), with pollen and macrofossil palaeoecological records frequently being used to reconstruct past climate and environmental change. For example, several Holocene pollen-inferred temperature reconstructions exist for northern Fennoscandia (Bjune et al., 2004; Seppä et al., 2004; Sjögren and Damm, 2019), with some reconstructions showing significant variation from both the ice-core record and typical NW European seaboard reconstructions (Shala et al., 2017). However, understanding long-term vegetation dynamics from pollen is limited by plant productivity and fossil preservation (Clarke et al., 2020). For example, the taxonomic resolution of pollen analysis is frequently limited to family or genus level, and thus limits the application of indicator species or trait-based approaches (Seppä et al., 2004). The dominance of long-distance wind-dispersed grains in pollen analyses can also conceal local vegetation changes, providing ambiguous information about the local presence or absence of tree species in treeline regions (Ranta et al., 2006; Seppä et al., 2002). The over-representation of surrounding trees in boreal forests, particularly pine, can swamp other taxa (Birks, 2003; Birks and Birks, 2000). Thus, here we use sedimentary ancient DNA (*sed*aDNA) to reconstruct vegetation history.

The recent development and application of (*sed*aDNA) to quantify species composition and real plant diversity presents new opportunities for increasing species richness and improving environmental reconstructions. *Sed*aDNA can identify more plants to species level (Alsos et al., 2016), particularly common arctic and boreal forbs (Clarke et al., 2020), thus a more complete, and potentially trait-based, reconstruction signal of local vegetation change can be obtained. This is important in climatically sensitive ecotones, such as the arctic-boreal treeline, where the presence of forest can influence local atmospheric and climatic feedback mechanisms, trophic interactions, and ecosystem functioning (Artaxo et al., 2022; Bjorkman et al., 2020; Bonan et al., 1992; Mekonnen et al., 2021). Here, we trial plant *sed*aDNA for reconstructing past temperature trends using current plant temperature minima and trait-based ecological preferences (Alsos et al., 2022; Elliott et al., 2023).

Chironomids have been widely recognised as valuable palaeoenvironmental indicators, with changes in taxonomic composition reflecting changes in temperature (Axford et al., 2017; Eggermont and Heiri, 2012; Engels and Cwynar, 2011). However, during periods of low magnitudes and rates of climate change, such as the Holocene (Mayfield et al., 2021; Wolff et al., 2010), chironomid assemblages have been shown to be responsive to other environmental or in-lake variables such as pH, nutrient input, dissolved oxygen, lake depth, total phosphorus and aquatic vegetation (Brooks, 2006; Langdon et al., 2006; Quinlan and Smol, 2001; Velle et al., 2005). Such drivers can also cause changes in ecosystem structure and functionality; for example, through acidification and nutrient supply (Heiri and Lotter, 2003; Il'yashuk et al., 2005; Velle et al., 2010). Boreal lakes can undergo natural acidification during the early Holocene due to soil development and colonisation by acidifying vegetation (Birks et al., 2000) and bedrock weathering (Boyle et al., 2013). Lake pH is known to have a strong influence on chironomid assemblages (Brooks, 2006; Velle et al., 2005). Lake nutrient availability can be increased by catchment soil and vegetation development (Bradshaw et al., 2005; Renberg et al., 1990). Changes in nutrient supply can influence the chironomid communities (Langdon et al., 2006). Thus, changes within the catchment can strongly influence water quality and the chironomid community.

Here, we investigate lake catchment and ecosystem development from a small interior lake at the northern extent of the boreal forest in north-east Norway and attempt to derive Holocene summer temperature reconstructions. This lake was selected because of its geographical location at the climatically sensitive northern limit of the boreal ecotone. We use sedimentological proxies (scanning X-ray fluorescence, magnetic susceptibility and loss-on-ignition) as indicators of changing landscape dynamics, *sed*aDNA as a record of vegetation development, and chironomids as a proxy for lake ecosystem. As it is not uncommon for chironomid temperature reconstructions to be affected by variables other than temperature during the Holocene, we test whether chironomids provide a realistic proxy record for temperature change at this site. We explore whether plant-based temperature reconstructions might be more reflective of temperature during this period and provide one of the first attempts at using plant *sed*aDNA as a tool to reconstruct past temperatures. Thus, here we present, for the first time, combined *sed*aDNA vegetation and chironomid analyses reconstructing Holocene climate and environmental dynamics.

2. Methods

2.1. Site description

Horntjernet (69.34919 N, 29.49156 E) is a small (1.19 ha), triangular lake located to the north of the Øvre Pasvik National Park in the Bácheveaj/Pasvikdalen valley, and west of the Pasvik River that forms the Norwegian-Russian border (Fig. 1). The lake has a small, low relief catchment (0.15 km^2) that drains into Hasetjørna Lake via the Skjellbekken River system. Situated at 88 m above sea level and 36 m above the main river valley, the lake is unlikely to have received direct inputs from the river during the mid-late Holocene although it was probably connected in the early Holocene given the relative uplift of this area (Romundset et al., 2011) The mean and maximum measured lake depths are 5.1 and 6.95 m, respectively. A nutrient index, calculated using rock type and weatherability (Rijal et al., 2021), indicates that the lake is currently nutrient poor. The bedrock is composed of sandstone with layers of phyllite, mica slate, and hornblende-rich gneiss overlain by thick moraine and eskers (NGU, 2023). The lake is a typical bedrock depression caused by glacial erosion. Although this part of the Fennoscandian shield was deglaciated relatively late (c. 12,000–11,000 cal yr BP, Hughes et al., 2016), the location of the site along a major valley led to glaciation prior to the Younger Dryas consistent with the basal radiocarbon date of c. 11,500 cal yr BP (Rijal et al., 2021). Modern catchment vegetation is dense pine forest and limited mire (for a species list see Rijal et al., 2021). The lake is fishless (to the authors' knowledge). Current local average climate conditions (1993–2019 CE) are boreal-arctic continental with a mean February temperature of −9.5 °C, mean July temperature of 13.8 °C, and an average annual precipitation of 524 mm (Pasvik National Nature Reserve, 2023). There is a large farm (Nordheim) 0.66 km west of the lake (external to the catchment), within an area of reclaimed mire (Kobbfossmyra), the closest part of which is still undergoing peatland reclamation. Although Pasvik is one of the least populated areas in Europe, it has a record of mid-late Holocene human land use including limited recent agriculture. Pasvik is one of the few areas in inland Finnmark that has received archaeological attention, including archaeological site excavation (Skandfer and Høeg, 2012). There is no archaeological evidence within the small Horntjernet catchment, thus it is unlikely that the lake has been impacted by regional human activities. See supplementary information for more detail on the regional archaeology.

2.2. Core retrieval, sampling, sedimentology and age-depth modelling

A 306 cm long, 10 cm diameter sediment core was retrieved from

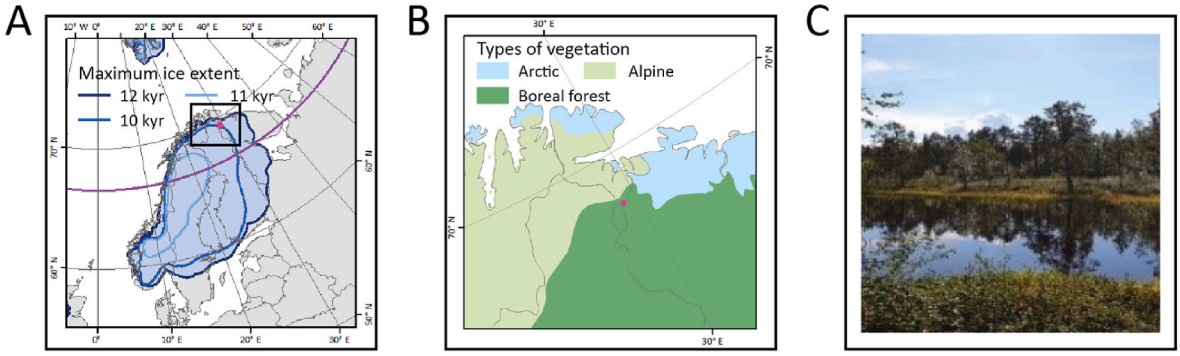

Fig. 1. Lake Horntjernet in the Pasvik valley, Finnmark, northern Norway. The lake lies at the edge of the maximum ice limit at 11,000 cal yr BP (Hughes et al., 2016) (A), and at the current northern extent of the boreal forest (European Environment Agency, 2016) (B). Photograph of Lake Horntjernet (C). Credit Inger Alsos.

Lake Horntjernet in March 2017 using a Nesje piston-corer (Nesje, 1992), as described in Rijal et al. (2021). Coring began at the surface or near-surface sediments, at 6.90 m water depth. The core was sectioned into three parts in the field, and stored at 4 °C. Each core section was longitudinally split, with one half used for destructive analyses and the other half retained for non-invasive scanning. Previously, the core was sampled for macrofossils where available, and for *sed*aDNA at 7 cm intervals (n = 44) as described in Rijal et al. (2021). The chironomid record (4 cm intervals, n = 71) has previously been analysed for community structural change (Mayfield et al., 2021). For this study, the core was sampled for loss-on-ignition (LOI) analyses (n = 72), taken concurrently with the samples for sed*a*DNA and chironomid analyses. All sampling was conducted within a dedicated ancient DNA facility at Tromsø Museum using sterile tools, a full bodysuit, facemask, and gloves, as described by Rijal et al. (2021).

The core sections were scanned for X-ray fluorescence (XRF), magnetic susceptibility (MS), and high-resolution colour imagery. The XRF scanning was performed every 5 mm at 10 kV using an Avaatech XRF core scanner, MS logging using a GEOTEK Multi Sensor Core Logger (MSCL-S) with a point sensor, and high-resolution imagery using a Jai L-107CC 3 CCD RGB Line Scan Camera (mounted to the XRF core scanner). Note that the cores were split at 66 cm and 186 cm. To minimise closed sum effects in the XRF area data, the raw peak element area was normalised against titanium (Ti) area, as Ti is considered to be a reliable indicator of allochthonous catchment inputs (Cohen, 2003), and thus by removing the allochthonous signal it is presumed the elements are indicating within lake changes. See Supplementary Dataset for the XRF and MS data.

Loss-on-ignition analyses were performed on 1–2 g of wet sediment sample, following Heiri et al. (2001) (see Supplementary Dataset). Samples were dried by heating to 105 °C overnight and the percentage of organic carbon was calculated by dividing the mass lost after heating the dried samples to 550 °C for 2 hours by the initial sample dry weight. The remaining sample was heated to 950 °C for 2 hours to calculate inorganic carbon and clay content.

The Bayesian age-depth model was previously constructed by Rijal et al. (2021) from 20 macrofossil-derived AMS radiocarbon dates. Here, we use an updated age-depth model calculated with the terrestrial IntCal20 curve (Reimer et al., 2020). We present sediment accumulation rates, calculated and plotted in *bacon* v2.3.4 (Blaauw and Christen, 2011).

2.3. Plant sedimentary ancient DNA (sedaDNA) dataset

The plant *sed*aDNA dataset was generated as part of a previous study (Rijal et al., 2021). This dataset (European Nucleotide Archive project PRJEB39329) consists of 44 samples from which DNA was extracted and amplified in eight PCR replicates (PCR repeats) using the vascular plant trnL p6-loop metabarcoding primers (Taberlet et al., 2012). Following Alsos et al. (2022), we used the count of PCR repeats (ranging from 1 to 8) for *sed*aDNA data quantification. This is a conservative quantification metric, and we note that it may underestimate the importance of the most read-abundant taxa. Data were merged based on functional group to show the proportion of *sed*aDNA repeats per functional group per sample. In the supplementary information, we also provide analysis outputs calculated from read percentages. Taxonomy and comments on plant ecology follow Lid and Lid (2005) and Elven et al. (2011).

2.4. Chironomid processing and taxonomy

Sediment samples were freeze-dried and deflocculated using 10% KOH for 18 min at 70 °C and passed through 180 and 90 μm sieves. Chironomid head capsules were picked individually from the residues using a Bogorov sorting tray and a mounted pin. The head capsules were air-dried and mounted in Euparal. Specimens were identified using the Brooks et al. (2007) and Wiederholm and Eriksson (1977) identification guides to sub-family level. At least 50 head capsules were counted for each subsample where possible (the minimum required to reduce errors within temperature reconstruction calculations, Heiri and Lotter, 2010). Two samples (depths 9.48 m and 9.52 m) with low head capsule concentration had total counts of 45 and 48. These were included in the analyses as the assemblage composition did not greatly differ from the consecutive samples and did not fall near a zone boundary.

2.5. Statistical analyses

Plant *sed*aDNA and chironomid data were analysed and plotted in R statistical software (R Core Team, 2019). For the plant assemblages, taxonomic richness was calculated as the total number of taxa recorded in each sample. For the chironomid assemblages, rarefaction was calculated as a metric of taxon richness. Taxa counts were rounded to integers and the minimum count sum was used to calculate rarefaction using the rarefy function in the *vegan* package (Oksanen et al., 2020).

Assemblage diagrams were created using the *Rioja* package (Juggins, 2015). Assemblage zones were created using cluster analysis from the *vegan* package (Oksanen et al., 2020), where dissimilarity indices were calculated using the *Bray-Curtis* method, with the bottom of the core as the base point. Broken stick analysis (using the bstick function in *vegan*), indicated 5 statistically distinct zones within the *sed*aDNA assemblage (Supplementary Figs. 2–3) and 6 statistically distinct zones within the chironomid assemblage (Supplementary Fig. 4). Zones were calculated from the dissimilarity indices using the *CONISS* (Constrained Incremental Sums of Squares) method. All DNA-derived datasets (PCR repeats and proportion of reads) were tested while establishing stratigraphic zones.

To assess the compositional change in the biological assemblages, Detrended Correspondence Analysis (DCA) was performed on the square root transformed *sed*aDNA repeat and chironomid data using the vegan

package (Oksanen et al., 2020).

2.6. Drivers of ecological change

To investigate the influence of precipitation and water availability on the landscape vegetation and lake water, local annual precipitation was reconstructed using the CHELSA TraCE21k climatic database (Karger et al., 2023), using a point extraction for the location of Horntjernet (Supplementary Fig. 5). A plant trait-based moisture requirement reconstruction was calculated using moisture requirement ecological indicator values from Tyler et al. (2021) (Supplementary Fig. 6). Ecological indicator values reflect modern species habitat characteristics (Körner, 2018), and past environmental conditions can be inferred based on the trait values of plants preserved in sedimentary records. The database constructed by Tyler et al. (2021) was developed specifically for Scandinavian regions. Mean realised plant moisture niche requirements were calculated for the plant taxa. Sample-wise mean moisture values were calculated for the proportion of PCR repeats, following Alsos et al. (2022). The moisture niche requirement is measured on a 12-point scale, where 3 = dry–mesic, 5 = mesic–moist, 7 = moist–wet, 9 = wet.

To assess whether changes in the landscape vegetation may have affected the lake water pH, trait-based pH classes were calculated for plant taxa identified to species level using species-specific ecological indicator values from Tyler et al. (2021). To do this, mean realised soil (water) pH niches (pH 1 to 8) were calculated for the plant taxa. Sample-wise mean pH values were calculated for the proportion of PCR repeats, following Alsos et al. (2022) (see Supplementary Fig. 7). The pH niche requirement is measured on an 8-point scale, where 2 = moderately-strongly acidic, 3 = moderately acidic (pH 4.5–5.5), 4 = moderately acidic - subneutral, 5 = subneutral (pH 5.5–6.5), 6 = subneutral-circumneutral, 7 = circumneutral (pH 6.5–7.5), and 8 = alkaline (pH > 7.5).

To assess whether the water pH may have influenced the chironomid assemblage change over time, the fossil chironomid samples were plotted passively on top of the ordination space of the Swiss-Norwegian chironomid calibration dataset (Heiri et al., 2011) with temperature and pH contours for comparison, using the functions *timetrack* (analogue package, Simpson and Oksanen, 2019) and *ordisurf* (vegan package, Oksanen et al., 2020). Goodness-of-fit analyses, using squared residual distance (Juggins and Birks, 2012), indicated that the Swiss–Norwegian chironomid calibration dataset was a good fit for the Horntjernet chironomid record (Supplementary Fig. 8). The Swiss-Norwegian chironomid calibration dataset contains chironomid assemblages from lakes situated on a range of climatic, geological and limnological conditions, including lakes with July air temperatures ranging from 3.5 to 18.4 °C and water pH values ranging from 4.7 to 8.8 (Heiri et al., 2011). We note that the authors identified July temperature as the primary influencing factor on the calibration dataset chironomid assemblages, and pH was not identified as a key driver. The abundance of acid tolerant taxa was compared to the plant trait-based pH reconstruction (Supplementary Fig. 9).

2.7. Temperature reconstructions

2.7.1. Chironomid-inferred temperature reconstruction

A local July air temperature reconstruction was calculated using the fossil chironomid dataset and the combined Swiss–Norwegian chironomid calibration dataset (Heiri et al., 2011). Goodness-of-fit analyses indicated that the Swiss–Norwegian chironomid calibration dataset was a better fit for the Horntjernet chironomid record than the Norwegian chironomid calibration dataset (Brooks and Birks, 2000, 2004) (Supplementary Fig. 8). To minimise variance, the chironomid percentage data were square root transformed prior to analysis. Outlier lakes within the calibration dataset were identified using Nonmetric Multidimensional Scaling (NMDS) and removed prior to analysis (Supplementary Fig. 10). A weighted averaging partial least squares regression model (WA-PLS, Ter Braak et al., 1993; Ter Braak and Juggins, 1993) was used to calculate the reconstructed temperatures, with R^2 = 1.49, RMSE = 0.84 °C and maximum bias 1.26 °C, as estimated using leave-one-out cross-validation. The temperature reconstruction was tested following the method published in Telford and Birks (2011), which aims to assess the significance of quantitative palaeoenvironmental reconstructions inferred from biotic assemblages and transfer functions. The reconstruction was compared to 999 randomised reconstructions to ascertain whether our reconstruction explained a greater proportion of the variance than the randomised datasets (Supplementary Fig. 11). The package *palaeoSig* v2.0-3 was used for the calculation (Telford, 2015). We repeated this test on early, mid-, and late Holocene subsets of the chironomid data (Supplementary Fig. 12). A temperature reconstruction performed using the Norwegian calibration dataset produced a comparable temperature reconstruction (Supplementary Fig. 13).

To investigate the influence of *Sergentia coracina*-type, a highly abundant chironomid in this record and typically a cold stenotherm, on the July air temperature reconstruction, a replicate reconstruction was calculated after removing *Sergentia coracina*-type from the assemblage (Supplementary Fig. 14). Considering the large abundance of *Sergentia coracina*-type within the record (<70 % in some samples), this reduced the head capsule count below the 50 head capsule threshold for 25 samples (lowest head capsule count 17.5). This could increase errors within temperature reconstruction calculation (Heiri and Lotter, 2001), and is used for testing purposes only.

2.7.2. Plant-inferred temperature reconstruction

A local July air temperature reconstruction was calculated using the plant *sed*aDNA record. Typically, pollen climate reconstructions are performed using pollen calibration datasets and WA-PLS regression (e.g. Bjune et al., 2004), similar to the method used for the chironomid temperature reconstruction. In the absence of a DNA-based plant calibration dataset, we used the following method. The plant record was filtered to retain aquatic and terrestrial taxa identified to species level (n = 65) (Supplementary Figs. 15–16). Mean and median values for the July temperature minima, mean, and optima were derived for these plant taxa from the CHELSA observational climate database (a large spatial climatology dataset for the years 1979–2013 CE, Karger et al., 2017) (Supplementary Fig. 17). For the PCR repeats, weighted mean July temperatures were calculated for each sample depth using the species mean minimum July temperatures, using the *weighted.mean* function in R. Due to the northerly location of Horntjernet, it was assumed that many taxa present were likely to be at the colder end of their temperature range. Temperature reconstructions calculated using the species median minimum, mean mean, and median mean July temperatures were calculated for comparison (Supplementary Figs. 18–19). A temperature reconstruction calculated using the proportion of *sed*aDNA reads and the species mean minimum July temperatures was calculated for comparison (Supplementary Fig. 20). The trend in the plant-inferred temperature reconstruction was compared to the turnover in the plant taxa (Supplementary Fig. 21).

The chironomid and plant-inferred temperature reconstructions were corrected for glacio-isostatic land-uplift using a relative sea level curve from the nearest coast (Nordkinn, from Romundset et al., 2011), which was scaled to the interior of Finnmark and the present height above sea level (60 m). The result was smoothed to simulate gradual uplift of the Fennoscandian dome (Mörner, 2003).

2.7.3. Plant trait-based temperature reconstruction

Trait-based thermal classes reflect the temperature conditions in which the plants were likely growing. Trait-based thermal classes were calculated using species-specific ecological indicator values (Tyler et al., 2021) to further investigate the ability of plant *sed*aDNA data to reconstruct Holocene climate change. The proportion of PCR repeats of

each trait category was calculated for temperature optimum, following Alsos et al. (2022) (Supplementary Fig. 22). Note, the trait values indicate vegetation classes, with larger values (max. 18) indicating colder temperatures (high arctic-alpine type vegetation) and smaller values (min. 1) indicating warmer temperatures (subtropical vegetation). The temperature optimum trait is based on the temperature regime at the centre of the geographic range of the species. For more information, see Tyler et al. (2021). For comparison between the plant-inferred and plant thermal trait-based reconstructed temperatures, see Supplementary Fig. 23.

2.7.4. Comparison with local and regional temperature reconstructions

Changes between the chironomid and plant community turnover (DCA axis 1 scores) and organic matter (LOI-550, %) were compared using Pearson's correlation (Supplementary Fig. 24). As DCA scores are non-dimensional, the correlation values were used to show association between variables, but not directional relationships.

The Horntjernet reconstructions were compared with other local and regional temperature reconstructions. A local July temperature reconstruction was calculated using the CHELSA TraCE21k climatic database using a point extraction for the location of Horntjernet (Karger et al., 2023). A chironomid-inferred July temperature record from Lake Loitsana, approx. 170 km to the south of Lake Horntjernet (Shala et al., 2017) (data extracted using WebPlotDigitizer), is used as a comparison for regional Holocene temperatures. The North Greenland Ice Core Project (NGRIP) oxygen isotope ($\delta^{18}O$) record is used as an independent proxy record of broad scale (Hemispheric/Atlantic) relative air temperature for the Holocene (Wolff et al., 2010). See Supplementary Figs. 25–36.

3. Results

3.1. Chronology and stratigraphy

A full Holocene sedimentary record is available from Lake Horntjernet, with the oldest radiocarbon date indicating that the basal sediments dated to c. 11,510 cal yr BP at 304.5 cm (Fig. 2). The sediment accumulation rate was generally low and curvilinear, but with some weak lamination and occasional single event (1–2 mm thick) in-washes, particularly between 230 and 80 cm (c. 8800 - 2600 cal yr BP). During the early Holocene, the mean sediment accumulation rate was approx. 0.027 mm/yr. There was a slight overall increase in the accumulation rate, with peaks between c. 10,500 to 10,100 cal yr BP (approx. 0.039 mm/yr) and 9000 to 8600 cal yr BP (approx. 0.049 mm/yr), and a decrease in the accumulation rate between c. 8500 to 8000 cal yr BP (approx. 0.017 mm/yr). In the mid-Holocene, the mean sediment accumulation rate was lower, approx. 0.019 mm/yr. There was a peak in sedimentation from 8000 to 7600 cal yr BP (approx. 0.051 mm/yr), after which the rate remained low, with a small peak around 4800 cal yr BP (approx. 0.030 mm/yr). In the late Holocene, the sedimentation rate had a general increasing trend. There was a peak at c. 3400 to 3000 cal yr BP (approx. 0.031 mm/yr), trough at c. 1500 to 1000 cal yr BP (approx. 0.024 mm/yr), and a peak at c. 1000 to 350 cal yr BP (approx. 0.049 mm/yr).

The basal sediments (prior to c. 10,550 cal yr BP, 306 - 286 cm) had a greater minerogenic (MS) and lower organic (LOI-550) content (Fig. 3). The lower 20 cm of sediment was paler in colour, transitioning from a yellowy-brown to darker brown. Elemental analysis, normalised against Ti, indicated greater K and lower Ca, Fe and Si content. Increased Ti indicates greater allochthonous material from the catchment. After c. 10,550 cal yr BP (285 cm), the sediment colour was dark brown and relatively stable. There was an abrupt decrease in the minerogenic component and increase in organic content (LOI-550). Elemental analysis indicated a lower K content and an increased Ca, Fe and Si. From c. 10,000 cal yr BP to present (260 - 0 cm), the minerogenic content was low (<3 %), organic carbon comprised approx. 50–70 % of the sediment, and the K content remained low. The relative stability in Ti after c. 9500 cal yr BP suggests a stable catchment with reduced allochthonous material in-washed. Fluctuations in the content of Ca/Ti, Fe/Ti, and Si/Ti were present though the core profile. Changes in the XRF values at 186 cm relate to the core break (decrease in Ca/Ti, Fe/Ti, and Si/Ti and a peak in Ti). There was a large decrease in the Ca/Ti, Fe/Ti and Si/Ti content near the top of the core profile, at c. 570 cal yr BP (30 cm). Inorganic carbon content (LOI %, 950 °C) was low throughout the

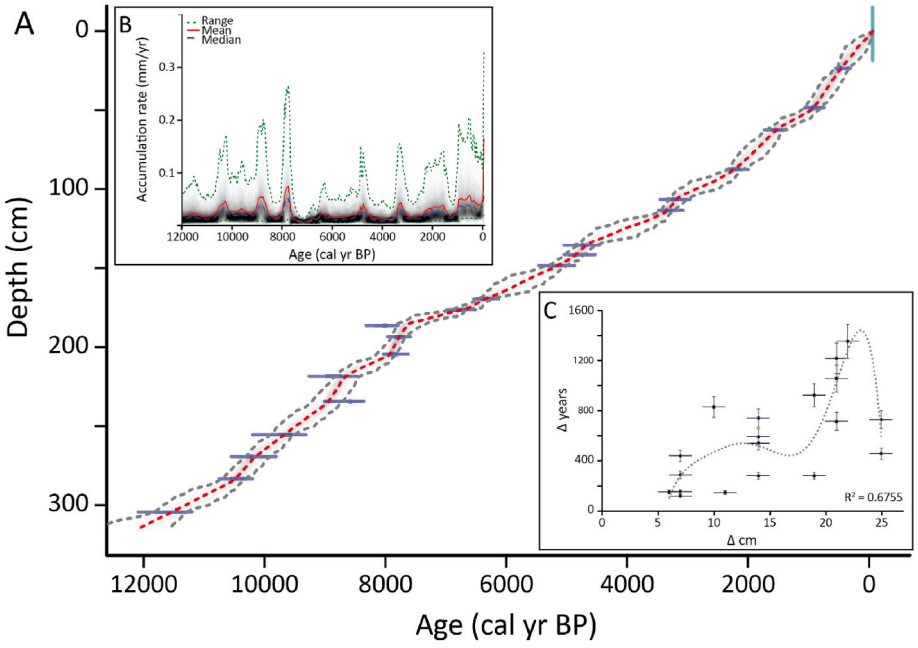

Fig. 2. The Horntjernet sediment age-depth model and accumulation rate. The age-depth model (A) was updated from Rijal et al. (2021), using the IntCal20 curve (Reimer et al., 2020). The accumulation rate plot (inset, B) indicates numerous fluctuations in the rate related to date spacing and an underlying irregular event-related rate. Spectral age plot (inset, C) showing a bimodal structure of higher SARs at 7–14 cm frequency and 19–22 cm supporting a pulsed SAR. The lowermost radiocarbon sample dated to c. 11,510 cal yr BP at 304.5 cm and the extrapolated basal date is 11,590 cal yr BP at 306 cm.

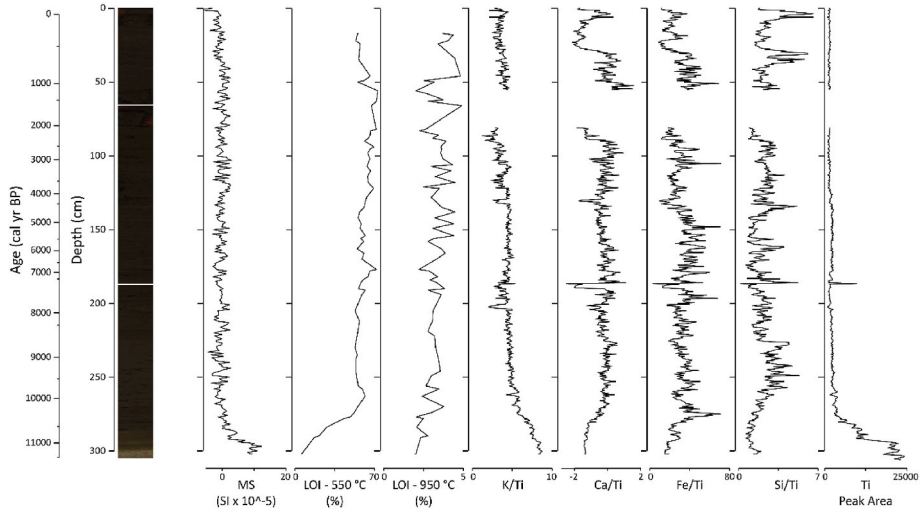

Fig. 3. Stratigraphy for Horntjernet. Core image, magnetic susceptibility (MS), organic (LOI-550, %) and inorganic (LOI-950, %) carbon content, and selected element (XRF) profiles are plotted against depth (cm), with correlated calibrated ages. Measurements of XRF were not taken between 55.5 and 80.5 cm due to an uneven sediment surface, and there is a fluctuation in the element values at the lower core break (186 cm). The peak area of the XRF elements were normalised by Ti, an allochthonous indicator. Changes in the Ti profile predominantly relate to catchment in-wash. The relative stability in Ti after the early Holocene suggests a stable catchment, thus, by normalising the other XRF elements against Ti, enables the changes in these elements to be attributed to within lake changes. Underlying geochemical data are presented in the Supplementary Dataset.

profile (<5%), with a slight rise in inorganic carbon/clay content at the onset of the Holocene.

3.2. Biostratigraphic records

3.2.1. Plant sedaDNA

A total of 141 taxa were identified: 8 taxa of trees (including *Salix* that may represent trees, shrubs and/or dwarf shrubs as well as *Betula* that may represent trees or shrubs), 2 shrubs, 15 dwarf shrubs, 43 forbs, 19 aquatic macrophytes, 16 graminoids, 13 vascular cryptogams, 21 bryophytes, and 4 taxa of algae (Supplementary Figs. 37A–C). Taxon richness ranged from 13 to 39 taxa, most of which were terrestrial taxa (range 9–34, Fig. 4). Aquatic macrophyte richness ranged from 1 to 9, and algae richness ranged from 0 to 3. There was a large turnover of taxon types in some functional groups, such as forbs, graminoids and aquatic macrophytes. CONISS analyses suggested four to five zones, depending on the dataset used (aquatic versus terrestrial taxa and proportion of reads versus proportion of PCR repeats) (Supplementary Figs. 2–3). All analyses identified boundaries at c. 10,400 cal yr BP. Analyses of terrestrial taxa identified boundaries at 8900, 7800, and 3300 cal yr BP. Analyses of aquatic taxa identified boundaries at 9800, 4700 (PCR repeats only), and 3300 cal yr BP (proportion of reads only).

Here, a summary is presented indicating the proportions of terrestrial and aquatic taxa, total taxon richness, and key taxa present in the assemblages (Fig. 4, Table 1). Trees and shrubs are grouped as several of the taxa (e.g. *Salix* and *Betula*) could have been trees or shrubs. Five assemblage zones are drawn using the main boundaries calculated from the proportion of repeats of terrestrial taxa: 10,400, 8900, 7800 and 3300 cal yr BP. The most recent sample is dated at c. 1980 CE.

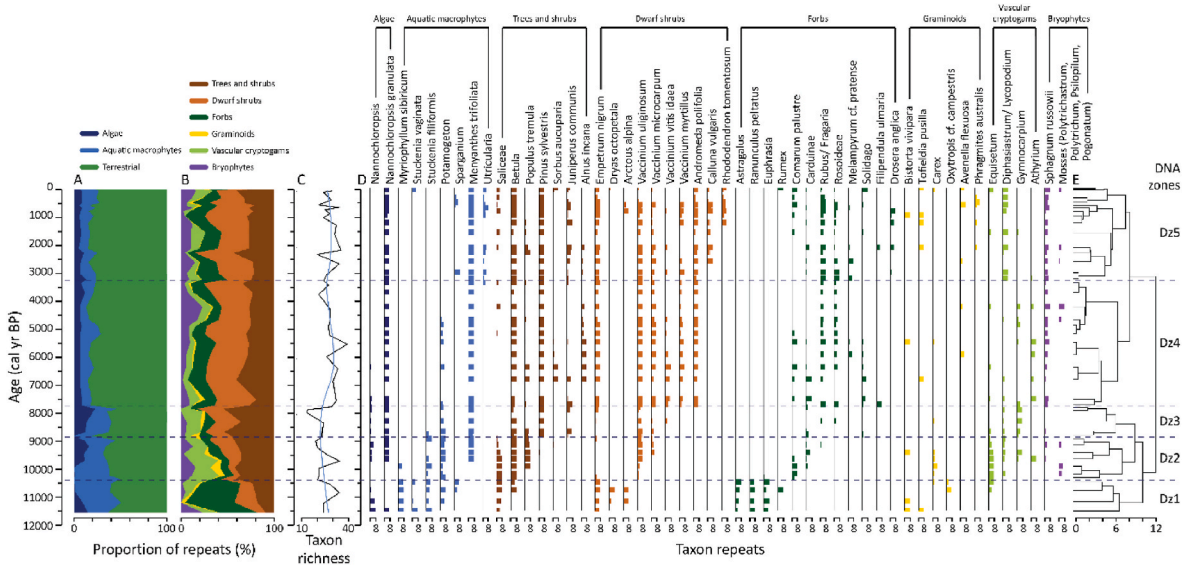

Fig. 4. Vegetation development reconstructed from Lake Horntjernet. Proportion of PCR repeats for terrestrial vascular plants, aquatic macrophytes and algae (A), and terrestrial plant functional groups (B). Taxon richness, with smoothed loess regression line in blue (C). Stratigraphic plot of most frequent taxa based on the number of detections of taxa in eight PCR replicates (D). Horizontal dotted lines indicate plant zones based on CONISS analysis of all taxa (E).

Table 1
Summary of plant assemblage zones.

Plant sedaDNA zone 1 (Dz1): Onset of the Holocene c. 11,500 - 10,400 cal yr BP
The vegetation at the onset of the Holocene was characterised by terrestrial plant taxa (approx. 49–63 %, predominantly forbs) and aquatic macrophytes (approx. 22–41%). The proportion of algae was low and decreased within the zone (approx. 1–15 %). Taxon richness was relatively high across the zone (mean 28, range 24–34). Forb taxa dominated the early plant record, including typical northern boreal/arctic taxa such as *Astragalus, Bistorta, Oxytropis,* and *Tofieldia*. The dwarf shrub taxon *Empetrum nigrum* had a strong early presence. The presence of the dwarf shrubs *Dryas octopetala* and *Arctous alpina* indicated some open habitat. Both Saliceae (tribe containing *Populus* and *Salix*) and *Betula* were present in this period, and most likely represent shrubs. Aquatic macrophytes present were *Stuckenia vaginata*, *Stuckenia filiformis*, *Myriophyllum sibiricum* and *Potamogeton*.
Plant sedaDNA zone 2 (Dz2): Early Holocene c. 10,400–8900 cal yr BP
The plant assemblages were dominated by terrestrial taxa (approx. 50–62 %, mainly vascular cryptogams and trees/shrubs) and aquatic macrophytes (approx. 38–50 %). Algae disappeared (<1 %). Taxon richness decreased (mean 20, range 20–21). Terrestrial taxa were dominated by Saliceae and *Betula*, likely representing shrubs. *Populus tremula* had a low presence towards the end of the zone. The dwarf shrubs of previous zone disappeared (*Dryas, Arctous*) or decreased (*Empetrum*) and were replaced by the more boreal *Vaccinium uliginosum*. The dwarf shrub *Vaccinium microcarpum,* typically restricted to peatlands, appeared at c. 9700 cal yr BP. Forb taxa decreased in overall presence, with a turnover in the taxon types present; *Astragalus*, *Euphrasia* and *Ranunculus peltatus* declined or disappeared, and Carduinae, Rosoideae, and *Rubus/Fragaria* appeared. The latter was most likely *Rubus chamaemorus,* which is common on mires/peatlands. There was an increase in graminoids (*Carex*), vascular cryptogams (*Equisetum* and *Diphasiastrum/Lycopodium*), and bryophytes (*Sphagnum* and other mosses).
Plant sedaDNA zone 3 (Dz3): Early/Mid-Holocene c. 8900 - 7800 cal yr BP
Dz3 was characterised by mainly terrestrial taxa (approx. 54–81 %) and aquatic macrophytes (approx. 15–34 %). Algae reappeared (approx. 0–23 %). Taxon richness was variable (mean 22, range 13–34). Trees and shrubs were the dominant types of terrestrial taxa. *Betula* remained present throughout the zone. Saliceae and *Populus tremula* disappeared while *Pinus sylvestris* appeared, suggesting a transition to pine forest. *Sorbus aucuparia* had low presence in two samples. *Juniperus communis* appeared in the middle of the zone. Dwarf shrubs were dominated by *Vaccinium* species and *Empetrum nigrum*. Forbs, graminoids, vascular cryptogams, and bryophytes had a low presence and similar composition to Dz2.
Plant sedaDNA zone 4 (Dz4): Mid-/Late Holocene c. 7800 - 3300 cal yr BP
This zone was dominated by terrestrial taxa (approx. 71–87 %, mainly trees/shrubs and dwarf shrubs). Aquatic macrophytes decreased in proportion (approx. 7–22 %). Algae remained present at low proportions (approx. 6–12 %). Taxon richness increased (mean 29, range 21–39). Trees/shrubs and dwarf shrubs were the dominant terrestrial taxa. *Betula* and *Pinus sylvestris* were present throughout the zone. *Populus tremula*, *Sorbus aucuparia*, and *Juniperus communis* were present in most samples. Saliceae re-appeared and *Alnus incana* appeared in the middle of the zone. A large variety of dwarf shrubs were present throughout the zone, with *Empetrum nigrum* and *Vaccinium* species continuing from Dz3. New dwarf shrubs arrived: *Vaccinium myrtillus* (common on acid soils and heathlands) and *Andromeda polifolia* (mainly found on mires). The forb composition was similar to Dz2 and Dz3. Graminoids, cryptogams, and bryophytes increased, including the taxon *Sphagnum*, throughout the zone. The plants do not indicate evidence of deforestation at c. 6950 cal yr BP, as evident in other local areas, such as Fosslund (Skandfer and Høeg, 2012).
Plant sedaDNA zone 5 (Dz5): Late Holocene c. 3300 cal yr BP to present
Terrestrial taxa remained dominant approx. 72–85 %, mainly trees/shrubs and dwarf shrubs), aquatic macrophytes (approx. 8–18 %) and algae remained present at low proportions (approx. 5–14 %). Taxon richness remained high (mean 28, range 20–35). Trees/shrubs and dwarf shrubs remained the dominant terrestrial taxa in the most recent zone. All tree/shrub taxa were present. Dwarf shrubs present in Dz4 remained present; while two new dwarf shrubs appeared in the record, *Calluna vulgaris* (first appearance c. 2500 cal yr BP) and *Rhododendron tomentosum* (first appearance c. 1200 cal yr BP). Forbs increased in presence; with the continuation of the forb taxa present in Dz4, *Rumex* re-appeared in the most modern sample, and the mire plant *Drosera anglica* appeared. Graminoids were present in low numbers, and *Phragmites australis* (a wetland grass) appeared in the record for the first time. Cryptogams and bryophytes were present in low numbers. There was a slight increase in plant diversity in the last 300 years (top of zone Dz5) associated with the appearance/re-appearance of *Stuckenia vaginata*, *Picea*, *Rumex*, *Carex*, *Avenella flexuosa* and *Phragmites australis*.

3.2.2. Chironomids

A total of sixty-four chironomid taxa were identified to genus or species-morphotype and chironomid taxon richness, as measured by rarefaction, ranged from 9 to 23. Six significant assemblage zones were identified by the CONISS analysis (Fig. 5, Table 2, Supplementary Fig. 4). The most recent sample is dated at c. 1780 CE.

3.2.3. Summary of Holocene environmental change

There was a strong coupling between the edaphic and biotic proxies in Lake Horntjernet; with changes in the plant and chironomid assemblages relating to changes in the sedimentology records (Fig. 6). In the early Holocene (c. 11,500 to c. 7800 cal yr BP), the DCA axis 1 scores indicated a large turnover (approx. 2.5 σ) in the plant and chironomid

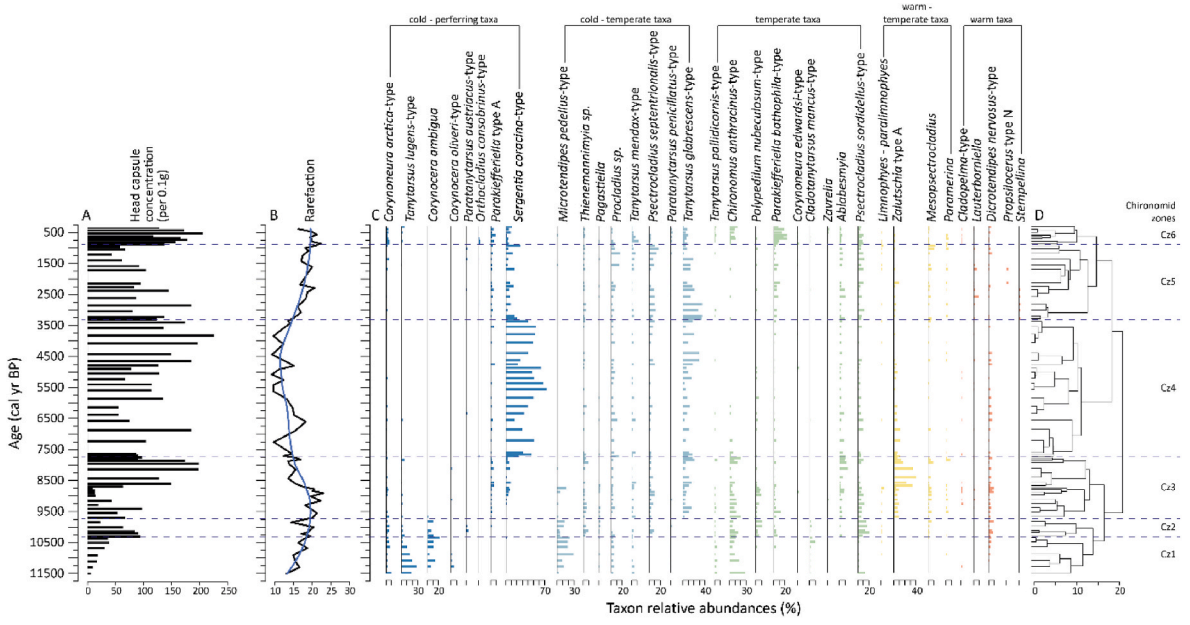

Fig. 5. Chironomid assemblage in Lake Horntjernet; head capsule concentration (number of heads per 0.1 g of freeze-dried sediment) (A), rarefied taxon richness, with smoothed loess regression line in blue (B) and relative abundances (percentages of the total) of the dominant chironomid taxa (C). Horizontal dotted lines indicate chironomid zones from the CONISS based dendrogram (D).

Table 2
Summary of chironomid assemblage zones.

Chironomid zone 1 (Cz1): Onset of the Holocene c. 11,500 to 10,*400 cal yr *BP
At the onset of the Holocene, the chironomid assemblages were dominated by cold stenothermic *Tanytarsus lugens*-type and cool-temperate taxa, such *as Corynocera ambigua* and *Corynoneura arctica*-type (Brooks et al., 2016; Brooks and Heiri, 2013). Other abundant taxa include *Microtendipes pedellus*-type (associated with coarse sediment and low organics) and *Chironomus anthracinus*-type (frequently a coloniser, able to withstand suboptimal conditions) (Brooks, 2006; Brooks et al., 2007). The chironomid head capsule concentration was low suggesting low productivity. Taxon richness was low at the start of the zone and increased through the zone (mean 16, range 13–19).

Chironomid zone 2 (Cz2): Early Holocene c. 10,400 to* 9800 cal yr *BP
Cold stenothermic taxa declined in abundance, such as *Corynocera ambigua*, *Corynoneura arctica*-type and *Tanytarsus lugens*-type. *Chironomus anthracinus*-type persisted. The most dominant taxon was *Psectrocladius sordidellus*-type, a temperate taxon often associated with macrophytes (Brodersen et al., 2001; Brooks et al., 2007). *Dicrotendipes nervosus*-type, also associated with macrophytes (Brooks et al., 2012b), increased in abundance. The head capsule concentration increased, suggesting a greater abundance of chironomid larvae present within the lake. Taxon richness increased throughout the zone, excluding the youngest sample (mean 18, range 14–20).

Chironomid zone 3 (Cz3): Early – Mid- Holocene c. 9800 to* 7800 cal yr *BP
Taxa associated with warmer, productive lakes were dominant in this early-mid- Holocene boundary zone, including *Tanytarsus glabrescens*-type, *Ablabesmyia*, *Dicrotendipes nervosus*-type, Mesopsectrocladius (*Psectocladius barbatipes*-type) and *Zalutschia* type A (Barley et al., 2006; Brooks, 2006; Brooks et al., 2007; Brooks and Heiri, 2013). *Sergentia coracina*-type arrived in the assemblage in low abundances. Head capsule concentration was variable, increasing towards the top of the zone. Taxon richness was high at the start of the zone and decreased after c. 8800 cal yr BP (mean 18, range 14–23).

Chironomid zone 4 (Cz4): Mid/Late Holocene c. 7800 to* 3300 cal yr *BP
This mid-Holocene zone was dominated by *Sergentia coracina*-type, a cold stenotherm (Brundin, 1949; Pinder, 1983), which is also acidophillic (Belle and Johnson, 2024; Wiederholm and Eriksson, 1977). *Tanytarsus glabrescens*-type was also abundant. *Chironomus anthracinus*-type disappeared from the assemblage at the start of the zone. *Zalutschia* type A declined in abundance and disappeared at the end of the zone. *Dicrotendipes nervosus*-type, *Psectrocladius sordidellus*-type, *Procladius* sp. and *Ablabesmyia* were present in low numbers throughout the zone. Head capsule concentration was relatively high, yet variable throughout the zone. Taxon richness was lowest in this zone (mean 13, range 9–18).

Chironomid zone 5 (Cz5): Late Holocene c. 3300 to* 800 cal yr *BP
Sergentia coracina-type decreased in abundance but remained present throughout the zone. Taxa which increased in abundance: *Tanytarsus glabrescens*-type (thermophilic, associated with productive, nutrient rich lakes with high LOI and DOC) (Brooks and Heiri, 2013; Perret-Gentil et al., 2024), *Parakiefferiella bathophila*-type (associated with warmer, more eutrophic lakes) (Brooks, 2006; Gouw-Bouman et al., 2019) and *Psectrocladius sordidellus*-type (temperate lakes, macrophytes, shallow waters, acidophilic) (Langdon et al., 2010; Luoto and Salonen, 2010; Nazarova et al., 2017). Head capsule concentration decreased throughout the zone, yet taxon richness increased (mean 18, range 14–21).

Chironomid zone 6 (Cz6): Late Holocene c. 800 to cal yr BP to present
In the most recent zone, *Parakiefferiella bathophila*-type increased in abundance, while *Sergentia coracina*-type, *Tanytarsus glabrescens*-type and *Psectrocladius sordidellus*-type remained constant. *Chironomus anthracinus*-type re-appeared in the assemblage. Head capsule concentration increased at the start of the zone and remained high. Taxon richness further increased (mean 20, range 16–22).

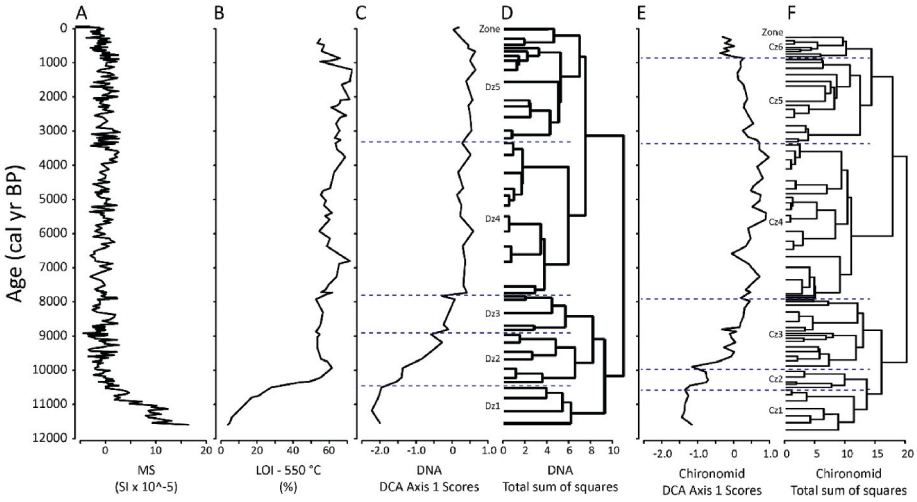

Fig. 6. Changing sediment type and assemblage composition at Horntjernet over the last c. 11,500 years. Magnetic susceptibility (MS) (A), loss-on-ignition (LOI-550, %) (B), *sed*aDNA plant DCA axis 1 scores (C), *sed*aDNA plant CONISS based dendrogram (D), chironomid DCA axis 1 scores (E), and chironomid CONISS based dendrogram (F). Plant and chironomid assemblage CONISS zones are marked on the corresponding DCA axis 1 score plots. The DCA axis 1 explained 37.9% and 27.2% of the variance for plants and chironomids assemblage, respectively.

assemblages as the sediment minerogenic content decreased and organic content increased. In the mid-Holocene (c. 7800 to 3300 cal yr BP), there was little directional change within the sediment composition (MS was low, LOI-550 fluctuated between 50 and 70 %), and the DCA axis 1 scores indicated little turnover in the plant and chironomid assemblages. In the late Holocene (c. 3300 cal yr BP to present), the sediment minerogenic content remained low, while the organic content remained high until c. 1200 cal yr BP, after which it decreased. In the plant record, the DCA axis 1 scores remained constant, with a small decrease in scores in the upper most sediments. The chironomid DCA axis 1 scores decreased slightly throughout the late Holocene, with a sharp decline in DCA axis 1 scores following the decline in organic content (c. 850 cal yr BP). The CONISS cluster analysis indicated one assemblage zone for the plant record and two assemblage zones for the chironomid assemblage in the late Holocene, suggesting the change in environmental conditions had a greater effect on the aquatic (chironomid) system than the terrestrial (plant) ecosystem. Pearson's correlation indicated a strong relationship between the organic matter content and turnover in the plant (0.823, p value < 0.000) and chironomid (0.760, p value < 0.000) assemblages (Supplementary Fig. 24).

3.3. Drivers of ecological change

The local annual precipitation reconstruction indicates an increase in precipitation at the onset of the Holocene (c. 12,000 to 11,500 cal yr BP) (Fig. 7A). Precipitation remains relatively stable between c. 11,500–9500 cal yrs BP, slightly decreases from c. 9500 to 8500 cal yrs BP, is reduced between c. 8400 to 8000 cal yrs BP, and then increases

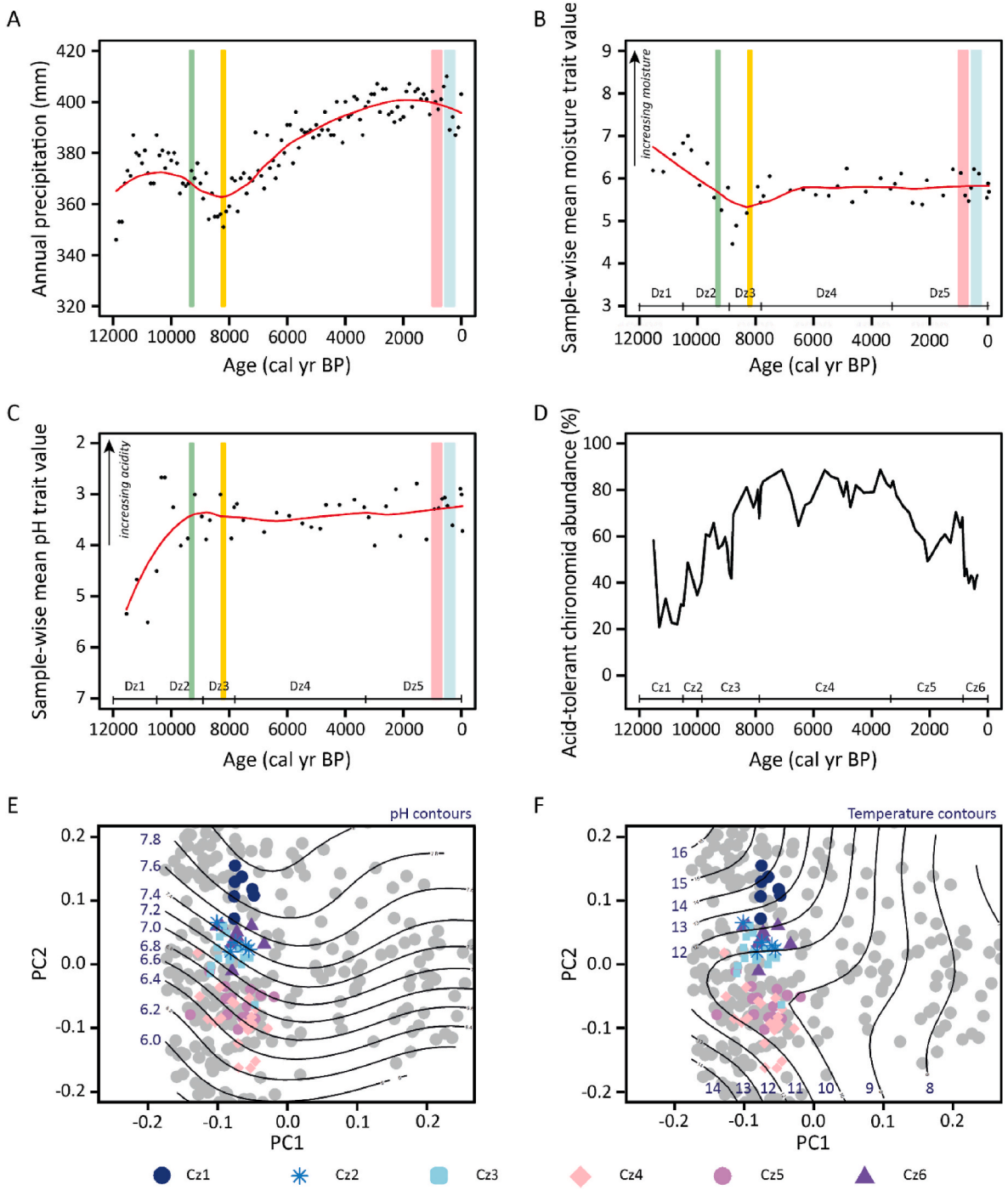

Fig. 7. Local annual precipitation reconstruction from the CHELSA TraCE21k database (Karger et al., 2023) (A). The plant trait-based moisture requirement reconstruction for the *sed*aDNA PCR repeats mean trait values, plant zones indicated along the x-axis. Moisture requirement is measured on a 12-point scale, with 3 = dry–mesic, 5 = mesic–moist, 7 = moist–wet, 9 = wet (B). Mean pH trait types for the plant taxa at Horntjernet through the Holocene, plant zones indicated along the x-axis. Note the reversed y-axis, where 3 = moderately acidic (pH 4.5–5.5), 5 = subneutral (pH 5.5–6.5), and 7 = circumneutral (pH 6.5–7.5) (C). Plant traits from (Tyler et al., 2021). Data points in grey, with smoothed loess regression line plotted in black. Total abundance (%) of acid tolerant chironomid taxa, with chironomid zones indicated along the x-axis (D). Chironomid samples plotted passively on the Swiss-Norwegian chironomid calibration dataset with pH (E) and temperature (F) contours. Samples are coded according to their assemblage zone. Climatic events indicated by vertical coloured lines; green - 9.3ka event (Rasmussen et al., 2007), yellow - 8.2ka (Rasmussen et al., 2007), pink - Medieval Climate Anomaly (MCA), and blue - Little Ice Age (LIA) (Mann et al., 2009; Wanner et al., 2008).

throughout the mid-late Holocene. There is a decrease in precipitation from c. 400 to 100 cal yrs BP. The majority (approx. 40–60%) of the precipitation fell during the summer months (Supplementary Fig. 5).

The plant trait-based moisture reconstruction indicated a greater proportion of plants preferring drier conditions during the early Holocene (c. 11,500–8200 cal yr BP) (Fig. 7B), as shown by the decrease in the mean moisture trait value (a lower value indicates that plant assemblage contains more plants with a lower water requirement). The mid-late Holocene indicates stability in the mean moisture requirement of the plants, with a mean of approx. 5.8 (indicating mesic-moist to moist). There was a greater proportion of plants with a higher moisture requirement in the mid-late Holocene, than in the early Holocene

(Supplementary Fig. 6).

In the early Holocene (c. 11,500 to 10,500 cal yr BP, zone Dz1), the plant trait-based pH reconstruction indicated the plant assemblages had a higher pH niche requirement; mean pH trait value 5, indicating sub-neutral soil approx. pH 5.5–6.5 (Fig. 7C). The remainder of the assemblages (c. 10,500 cal yr BP to present) had a lower pH niche requirement; mean pH trait value 3.3, indicating moderately acidic soil, approx. pH 4.5–5.5. There was an increase in plants with a moderately acidic soil preference at c. 10,500 cal yr, and an increase in plants with a moderately-strongly acidic soil preference at c. 7900 cal yr (Supplementary Fig. 7).

There was an increase in the abundance of acid tolerant chironomid taxa in zones Cz4 and Cz5 (Fig. 7D). The Horntjernet chironomid samples plotted across a pH gradient of 6.2–7.8 in the Swiss-Norwegian chironomid calibration dataset (Fig. 7F). Zone Cz1 contained chironomids at the neutral to alkaline pH range (pH 7.2–7.8). Zones Cz2, Cz3 and Cz6 plotted within the 6.8–7.4 pH range (with one exception at c. 8000 cal yr BP). Zones Cz4 and Cz5 plotted within the more acidic sample range, pH 6.2–7.0, suggesting the lake was more acidic during this time (c. 7800 - 825 cal yr BP). In comparison, the Horntjernet chironomid samples plotted within the warmer section (10–15 °C) of the temperature gradient in the chironomid calibration dataset (Fig. 7F). The taxon composition of Cz1 had greater taxa similarity with the warmest samples in the calibration dataset, suggesting a greater presence of warm-preferring chironomids. The taxon compositions of Cz4 and Cz5 were more similar to calibration samples at the cooler end of the gradient. Horntjernet chironomid zones Cz2, Cz3 and Cz6 plotted centrally within the temperature gradient.

3.4. Reconstructed temperatures

3.4.1. Chironomid-inferred temperature reconstruction

The chironomid-inferred July temperatures indicated an overall warming trend throughout the Holocene (Fig. 8A). Temperatures ranged between approx. 9.9 °C and 14.0 °C, with a mean temperature of approx. 12.1 °C. Relative to local modern July temperatures (13.8 °C), all but two values of the reconstructed temperature were cooler than today.

At the onset of the Holocene (Cz1, c. 11,500 to 10,400 cal yr BP) temperatures were variable, with a general increasing trend (approx. 9.9 °C–11.8 °C). Temperatures were approx. 2.0–3.9 °C cooler than today. The oldest sample was anomalously warm compared with the rest of the zone, likely due to the large presence of *Chironomus anthracinus*-type (28.2%). Temperatures continued to rise throughout the early Holocene (Cz2 and Cz3), to c. 8900 cal yr BP when temperatures were approx. 12.7 °C (1.1 °C cooler than today). At c. 8400 - 8100 cal yr BP, there was a approx. 1 °C relative summer cooling, compared to the rest of Cz2.

During the mid-Holocene (Cz4, 7800 to 3300 cal yr BP), the chironomid-inferred temperatures indicated initial cooling then warming. Between c. 7800 to 4700 cal yr BP, the mean inferred temperature was 11.7 °C and range was 11.2–12.3 °C (1.5–2.6 °C cooler than today). This is likely due to the large presence of *Sergentia coracina*-type (approx. 40–75 %), a taxon more commonly associated with cold temperatures. The presence of *Sergentia coracina*-type lowered the mid-Holocene reconstructed temperatures by up to 1.53 °C (Supplementary Fig. 14). Towards the end of the zone, reconstructed temperatures indicated a brief increase at c. 4600 - 4300 cal yr BP (approx. 13.5 °C), before decreasing again from c. 4100 to 3500 cal yr BP (approx. 12.5 °C).

In the late Holocene, temperatures were warmest in zone Cz5, with peaks at c. 3300 and 2300 cal yr BP (approx. 14.0 °C, 0.2 °C warmer than today). Temperatures were warm yet variable between c. 3300 and 1500 cal yr BP (mean 13.2 °C). Two samples, c. 1300 -1100 cal yr BP, had lower reconstructed temperatures (approx. 10.7 and 11.4 °C, 3.1 to 2.4 °C cooler than today). The remaining samples ranged between approx. 11.6 and 13.0 °C; 2.2 to 0.8 °C cooler than today. The most recent sample (c. 240 cal yr BP or c. 1780 CE) was approx. 12.3 °C, 1.5 °C cooler than today.

We note that the Horntjernet chironomid-inferred reconstruction did not pass the significance test recommended by Telford and Birks (2011) (Supplementary Fig. 11). This is possibly due to the variability of temperature change within the reconstructed temperatures compared to the model validation checks ($R^2 = 1.49$, RMSE = 0.84 °C and maximum bias 1.26 °C). There was 4.0 °C of temperature change across the whole Horntjernet chironomid-inferred temperature record, with 3.1 °C of variation in the early Holocene reconstructed temperatures, 2.4 °C of variation in the mid-Holocene reconstructed temperatures, and 3.3 °C of variation in the late Holocene reconstructed temperatures. When the Telford and Birks (2011) test was repeated on subsets of temperature record, the tests also failed (Supplementary Fig. 12), likely due to the small number of samples (early Holocene zones Cz1 - Cz3 n = 28, mid-Holocene zone Cz4 n = 21, late Holocene zones Cz5 - Cz6 n = 22). Other regional Holocene chironomid reconstructions also do not pass the test, likely also due to relatively low variation in the reconstructed Holocene July temperatures (Il'yashuk et al., 2013; Luoto et al., 2014b). Other studies do not refer to the test (Engels, 2021; Shala et al., 2017). Here, we consider our reconstruction with caution and alongside other palaeoecological and environmental evidence (Brooks et al., 2012a).

3.4.2. Plant-inferred temperature reconstruction

The plant-inferred July temperatures indicated an overall cooling trend throughout the Holocene, with no early Holocene warming (Fig. 8B). Temperatures ranged between approx. 11.1 °C and 12.2 °C, with a mean temperature of 11.5 °C. Relative to local modern July temperatures (13.8 °C), the reconstructed temperatures were approx. 1.6–2.7 °C cooler than today. Reconstructed temperatures had greater variation in the early Holocene, from c. 11,500–7800 cal yr BP (assemblage zones Dz1, Dz2 and Dz3). The mid- and late Holocene, from c. 7800 to 800 cal yr BP was cooler with less variation; mean 11.4 °C, range 11.1–11.7 °C (approx. 2.1–2.7 °C cooler than today). The most recent samples showed a peak in temperature of 11.7–11.9 °C at c. 500 to 30 cal yr BP (approx. 1.9–2.1 °C cooler than today), before cooling in the most recent sample to 11.2 °C (approx. 2.6 °C cooler than today).

The reconstructed plant temperatures had greater variation in the early Holocene, from c. 11,500–7800 cal yr BP (zones Dz1, Dz2 and Dz3). In these zones, the total number of plant species used in the temperature reconstruction varied between 5 and 14, with a large turnover in the taxa type. For example, in Dz1 48% of all repeats were aquatic macrophytes, c. 24% forbs, c. 20 % dwarf shrubs, with no trees/shrubs, while in Dz3, 32% of repeats were aquatic macrophytes, 32% were trees/shrubs and 31% were dwarf shrubs (Supplementary Fig. 16). The aquatic taxa had a minimum July temperature range of 11.1–13.9 °C, compared to dwarf shrubs with minimum July temperatures of 6.8–13.3 °C, and trees/shrubs with minimum July temperatures of 12.0–13.3 °C (Supplementary Fig. 17, Karger et al., 2017). Thus, as the proportion of aquatic taxa decreased, the temperature reconstruction produced a cooling trend. In zones Dz4 and Dz5, the dominant taxa used in the temperature reconstruction were dwarf shrubs (54 % and 50 %, thermal range 6.8–13.3 °C), followed by trees/shrubs (26 % and 25 %, thermal range 12.0–13.3 °C). This consistent dominance and little turnover of dwarf shrub and tree/shrub taxa likely had a stabilising effect on the temperature reconstruction. The cooler mid-late Holocene temperatures (11.1–11.9 °C) are likely influenced by the persistence of *Vaccinium uliginosum* and *Empetrum nigrum* and appearance of cold-tolerant taxa (e.g. *Athyrium disentifolium*), and a reduction in aquatic taxa with warmer thermal optima (Supplementary Figs. 21 and 22).

3.4.3. Plant trait-based temperature reconstruction

The plant thermal trait-based reconstruction specifies rapid early Holocene warming, with zone Dz3 indicating a thermal maximum (9700–7800 cal yr BP) (Fig. 8C). In the mid-Holocene (c. 7800 to 3300 cal yr BP, zone Dz4), the temperature regime was slight cooler, yet

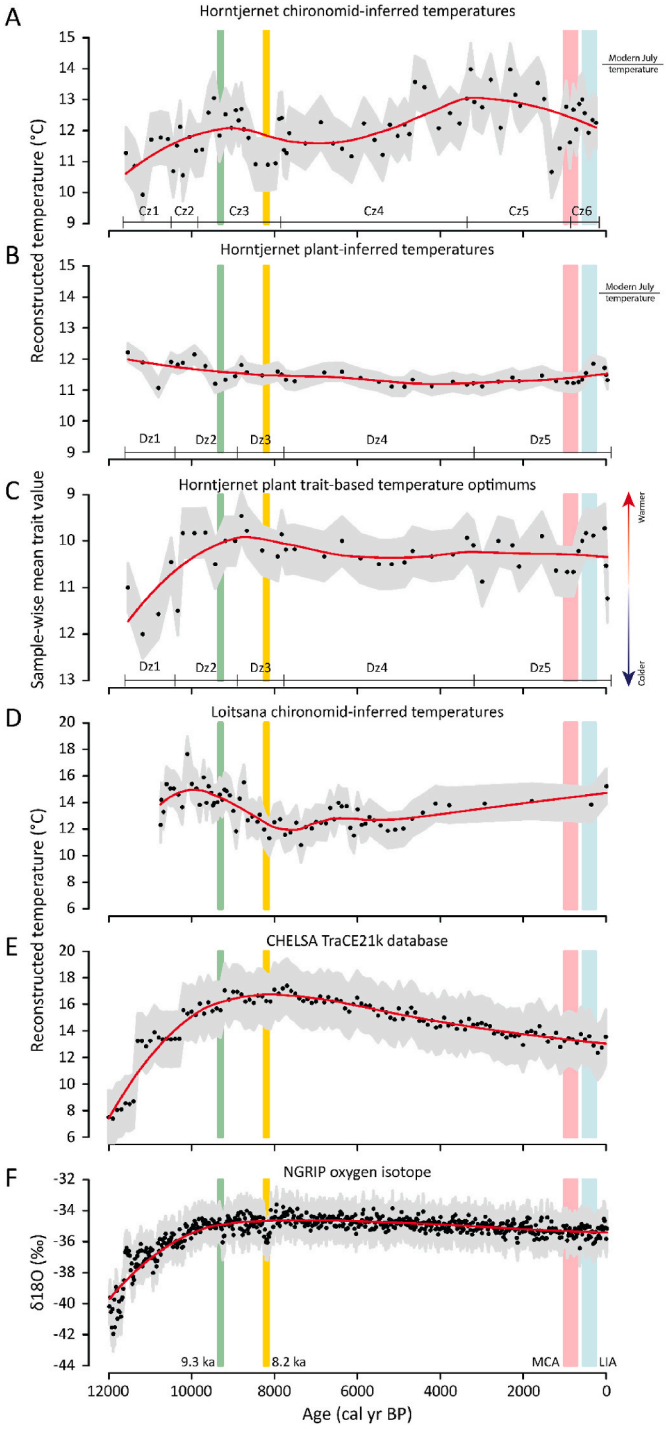

Fig. 8. Local and regional Holocene temperature reconstructions. Chironomid-inferred July temperature reconstruction from Lake Horntjernet (A). Plant-inferred July temperature reconstruction calculated using PCR repeats (B). Local modern (1993–2019 CE) mean July temperature is 13.8 °C. Plant thermal trait-based calculations of the Holocene temperature trend (C). Note the reverse scale of the temperature optimum (y-axis) where higher values indicate high arctic/alpine plants and lower values indicate temperate plants. Assemblage zones are indicated along the x-axis. Other local and regional temperature reconstructions are included for comparison; a chironomid-inferred July temperature record from Lake Loitsana (Shala et al., 2017) (D), a local CHELSA TraCE21k calculated July temperature reconstruction (Karger et al., 2023) (E), and the NGRIP oxygen isotope ($\delta^{18}O$, ‰) record spanning the Holocene (Wolff et al., 2010) (F). Lower isotopic values are indicative of lower temperatures. Dates corrected to cal yr BP from years B2K (ages relative to 2000 CE), following Wolff et al. (2010). Smoothed loess regression (span = 0.5) lines plotted in red. Standard deviation is used as a descriptive error envelope (in grey). Climatic events indicated by vertical coloured lines; green - 9.3ka event (Rasmussen et al., 2007), yellow - 8.2ka (Rasmussen et al., 2007), pink - Medieval Climate Anomality (MCA), and blue - Little Ice Age (LIA) (Mann et al., 2009; Wanner et al., 2008).

stable. In the late Holocene (c. 3300 cal yr BP to present, zone Dz5), the temperature regime remains cool, yet increases in variability. The temperature regime in the most recent samples indicate a slight cooling (c. 1200 to 800 cal yr BP), then warming (c. 500 to 30 cal yr BP), and decrease towards modern times (c. 30 cal yr BP to c. 1980 CE). This trend has some visual comparisons to the plant-inferred July temperature record (Supplementary Fig. 23).

4. Discussion

Holocene climatic amelioration occurred rapidly, with relatively high magnitude, climatic warming following deglaciation (Aarnes et al., 2012; Birks and Birks, 2008). The palaeoenvironmental evidence from Lake Horntjernet is typical of the region: showing local climatic amelioration with a rapid rise in organic lake sediment, high turnover of plant and chironomid taxa, change from a dominance of arctic-alpine plants to temperate plants, and change from cold stenothermic chironomid taxa to those preferring warmer, more productive lakes. Thus, to some degree, we would expect the biological temperature reconstructions to reflect local temperature change. Here, the chironomid-inferred July temperatures show early Holocene warming, cooler mid-Holocene temperatures, a mid-late thermal maximum, and a more recent cooling trend. The plant-inferred July temperature curve (based on current plant temperature minima) showed little change over the Holocene, whereas the trait-based temperature trend reconstruction indicated rapid early Holocene warming, with stable mid-late Holocene temperatures.

4.1. Rapid climate amelioration during the early Holocene (c. 11,600–7800 cal yr BP, plant zones Dz1-3 and chironomid zones Cz1-3)

4.1.1. Landscape development following deglaciation

The Horntjernet sediment record preserves an environmental archive from the onset of the Holocene (from c. 11,600 cal yr BP), indicating the lake started accumulating catchment sedimentation soon after deglaciation (c. 12,000–11,000 cal yr BP, Hughes et al., 2016). The sedimentological proxy evidence indicates a cool, open environment at the onset of the Holocene (11,500 to 10,400 cal yr BP), with highly minerogenic sediments and low organic matter content. The terrestrial plant record (Dz1) was dominated by low arctic to boreal terrestrial taxa (mainly forbs, approx. 25 %). Woody taxa like Saliceae (tribe containing *Populus* and *Salix*) and *Betula*, most likely representing shrubs, and dwarf shrubs (*Empetrum nigrum*) were present from the start of the record, suggesting early soil development. This is congruent across northern Norway, with local pollen records also indicating an early presence of Saliceae and *Betula*, e.g. Varanger Peninsula at c. 10,700 cal yr BP (Brown et al., 2022; Clarke et al., 2019) and Andøya at c. 10,520 cal yr BP (Birks, 2015).

The sedimentological record indicates rapid climatic amelioration (c. 11,000–9800 cal yr BP); organic matter content increased rapidly while minerogenic content decreased indicating soil development and more vegetation on the landscape. The plant community continued to develop, with a rapid turnover in taxa present (approx. 2σ) and an increase in the proportions of tree and shrub taxa (approx. 23%, Dz2). Saliceae and *Betula* persisted on the landscape. *Populus tremula*, a tree species often found in cool temperate and boreal regions, appeared on the landscape. This likely indicates the localised arrival of trees. Under the current *sed*aDNA metabarcoding approach, Saliceae and *Betula* cannot be identified to species-level, as the targeted barcode region is not species-specific (Wagner et al., 2021). However, *Betula pubescens* (tree birch) and *Betula nana* (dwarf birch) macrofossils were both found in the Early Holocene (10,500–8900 cal yr BP) in northern Fennoscandia (Bjune et al., 2004), thus demonstrating that *Betula* trees could be established by this time. The presence of *Carex*, *Equisetum*, and mosses suggests that the vegetation development not only reflects warmer temperatures, but also increased precipitation, congruent with the rise in local annual precipitation. Other vegetation studies have indicated increased temperatures and precipitation during the early Holocene in northern Norway (e.g. Birks et al., 2012).

The sedimentological record indicates environmental stability; low and constant minerogenic content and relatively high and constant organic matter content (c. 9800 to 7800 cal yr BP). The plant community continues to develop; Saliceae and *Populus tremula* disappeared from the record and were replaced with *Pinus sylvestris*. The arrival of *Pinus* is consistent with other studies; *Pinus* stands were present by c. 8500 cal yr BP in central Troms (Jensen et al., 2002), and c. 8400 cal yr BP on the Varanger Peninsula (Clarke et al., 2019), suggesting the regional development of pine woodlands. Taxa preferring, or tolerating, moderately acidic soils increased in abundance; *Vaccinium uliginosum* became the dominant dwarf shrub, and *Vaccinium microcarpum* and *Vitis idaea* taxa appeared. This indicates the catchment transitioned into a wooded, heathland, with more acidic soils. There was a decrease in taxon richness between c. 8300 - 7900 cal yr BP, with a brief decrease in the abundance of trees/shrubs (from approx. 33 %–21 %) and increase in dwarf shrubs (from approx. 13 to 16 %) and forbs (from approx. 3% to 7 %), perhaps indicating a response to the 8.2 ka event. There was a small peak in *Juniperus communis* at c. 7900–7700, possibly linked to a cooler or wetter period following the 8.2 ka event. A *Juniperus* event in association with the 8.2 ka event is observed elsewhere in Fennoscandia (Salonen et al., 2024; Seppä et al., 2002).

4.1.2. Lake formation and development

The early prominence of aquatic plant taxa suggests suitable in-lake growing conditions (Dz1), e.g. with clear water conditions for the growth of fully submerged plants such as *Myriophyllum sibiricum*, *Stuckenia filiformis*, *Stuckenia vaginata*. A well-developed aquatic community has been reported in lakes across Northern Norway, between 12,900 and 10,000 cal yr BP (Alsos et al., 2022; Väliranta et al., 2015). Aquatic macrophytes have fundamental roles within lake systems, providing habitats and food for a range of organisms, and promoting biogeochemical cycling, thus, the early appearance of aquatic macrophytes advances the development of the ecological structure and function of the lake (Bennion et al., 2018; Revéret et al., 2023). The chironomid community reflects a cool, open catchment with low in-lake productivity; head capsule concentration is low, and dominant taxa include cold stenothermic chironomid taxa (*Corynocera ambigua*, *Corynoneura arctica*-type and *Tanytarsus lugens*-type), taxa associated with minerogenic sediments and low organics (*Microtendipes pedellus*-type) and early coloniser *Chironomus anthracinus*-type (Brooks, 2006; Brooks et al., 2007, 2016; Brooks and Heiri, 2013). As the climate warmed and the environment developed (c. 10,300–9800 cal yr BP), there was a continued large presence of macrophytes (Dz2) and an abrupt rise in chironomid head capsule concentration (Cz2) indicating an increase in lake productivity. The decrease of cold stenothermic taxa (*Corynocera ambigua*, *Corynoneura arctica*-type and *Tanytarsus lugens*-type), and increase in more temperate (*Chironomus anthracinus*-type and *Psectrocladius sordidellus*-type) and warm (*Dicrotendipes nervosus*-type) taxa indicated a change in the chironomid community in response to warming temperatures. These temperate-warm taxa can also be associated with macrophytes (Langdon et al., 2010), the most abundant plant functional group at this time (38–50%).

The sediment record indicated environmental stability and woodlands in the catchment by c. 9800 to 7800 cal yr BP, however, in the aquatic system there was a turnover in the aquatic taxa. *Myriophyllum sibiricum*, *Stuckenia filiformis*, *Stuckenia vaginata* declined and disappeared, possibly indicating an increase in turbidity within the lake, as catchment productivity increased. There was an increase in the sediment accumulation rate between c. 9000 to 8600 cal yr BP, suggesting greater allochthonous material in-wash. A reduction in water clarity is supported by the arrival of the aquatic plant *Menyanthes trifoliata*, which has leaves above the water surface, an adaptation which promotes photosynthesis. The chironomid assemblage (Cz3) was dominated by taxa associated with warmer, productive lakes, suggesting increased lake

productivity (e.g., *Tanytarsus glabrescens*-type, *Ablabesmyia*, *Dicrotendipes nervosus*-type, *Mesopsectrocladius* (*Psectocladius barbatipes*-type) and *Zalutschia* type A (Barley et al., 2006; Brooks, 2006; Brooks et al., 2007; Brooks and Heiri, 2013). The increase in *Zalutschia* type A, which is also acidophilic (Brooks et al., 2007), towards the upper end of Cz3 could signify the lake starting to become more acidic. There were brief changes in the chironomid assemblages between c. 8400 and 8100 cal yr BP, likely representing the 8.2 ka event; for example, *Psectrocladius septentrionalis*-type (typically associated with cooler temperatures) increased in abundance. Changes in chironomid community have been identified in other regional records; northern Fennoscandia (Korhola et al., 2002; Antonsson et al., 2006), and Kola Peninsula (Il'yashuk et al., 2013).

4.1.3. Early Holocene warming

The chironomid-inferred temperature record indicates early Holocene temperature increases with a magnitude of 3.1 °C and a range of 9.9–13 °C. This is comparable to other regional chironomid-inferred temperature records, which calculated early Holocene temperature changes with a magnitude of approx. 2–3 °C, for example, approx. 11–12 °C in northern Norway (Brooks and Birks, 2000), approx. 10–12 °C in northern Finland (Luoto et al., 2014a), approx. 9–11 °C in northern Fennoscandia (Korhola et al., 2002), and approx. 9–12 °C in the Kola Peninsula (Il'yashuk et al., 2013). There was a relative 1 °C decrease in temperatures at c. 8400 - 8100 cal yr BP in the Horntjernet chironomid-inferred temperature record, likely relating to the 8.2 ka event (Rasmussen et al., 2007). Brief cold periods of similar magnitude at c. 8200 cal yr BP have been identified in chironomid-inferred temperature reconstructions from Fennoscandia (Antonsson et al., 2006; Korhola et al., 2002) and Kola Peninsula (Il'yashuk et al., 2013). The Lake Loitsana chironomid-inferred July temperature reconstruction (Fig. 8D, Northern Finland, Shala et al., 2017) indicated a greater magnitude (approx. 4.6 °C) of temperature change during the early Holocene, with slightly warmer temperatures, approx. 11.3–15.9 °C, with a maximum temperature of 17.6 °C (perhaps an outlier) occurring at c. 10,100 cal yr BP. There was no statistical correlation between the Horntjernet and Loitsana chironomid-inferred temperature reconstructions (Supplementary Fig. 28), although the Lake Loitsana record also indicated a decrease in temperature at c. 8200 cal yr BP. The CHELSA Trace21ka July temperature reconstruction indicated abrupt early Holocene warming, similar to the Horntjernet chironomid-inferred temperature reconstruction, however the CHELSA Trace21ka July temperature reconstruction suggested a c. 8 °C magnitude of temperature change in c. 2000 years, more similar to temperature changes experienced of a glacial to interglacial scale (Capron et al., 2014). There was a moderate correlation between the early Holocene Horntjernet chironomid temperature and CHELSA Trace21ka July temperature reconstructions (Pearson's correlation = 0.467, p value = 0.012, Supplementary Fig. 29), and NGRIP $\delta^{18}O$ record (Pearson's correlation = 0.517, p value = 0.005, Supplementary Fig. 30). Thus, the Horntjernet chironomid-inferred July temperature reconstruction has a similar temperature range to other published records and follows the general expected climatic trends during the early Holocene (early Holocene warming and 8.2 ka cooling).

The plant-inferred July temperature reconstruction indicated cooler than present temperatures (approx. 11.1 and 12.2 °C) with a decreasing trend in the early Holocene. Other published pollen-inferred temperature reconstructions indicate rising temperature trends in the early Holocene, with magnitudes of change (approx. 3 °C) and temperature ranges comparable to the chironomid records, e.g. approx. 9–12 °C in northern Norway (Bjune et al., 2004, 2010) and approx. 11–14 °C in northern Finland (Shala et al., 2017). Thus, the Horntjernet plant-inferred July temperature reconstruction is within the same temperature range, albeit less variable, as other published records. This supports the assumption made when calculating the temperature reconstruction; that many taxa present were likely at the cooler end of their temperature range due to the northerly location of Horntjernet.

The early Holocene Horntjernet plant-inferred temperature reconstruction was strongly affected by the dominance of macrophytes. Other Scandinavian plant-inferred July temperature reconstructions were calculated using fossil pollen records and modern pollen-climate calibration datasets which did not include aquatic pollen (Bjune et al., 2004; Seppä et al., 2004). Aquatic taxa are thought to be good climate indicators and have been used previously for Holocene summer temperature reconstructions (Väliranta et al., 2015). However, in this record, it is likely that the presence of aquatic taxa caused an overestimation of the early Holocene temperatures. A plant macrofossil-based temperature reconstruction from Lake Loitsana (Shala et al., 2017), calculated using the remains of aquatic and wetland plants also produced warmer than expected July temperatures during the earliest part of the Holocene. Removing the macrophytes from the Horntjernet temperature calculation decreased the temperatures, however produced more variable values due to the poor species richness; 6–13 species (see Supplementary Fig. 19). As the presence of macrophytes decreased in the Horntjernet record, the reconstructed temperatures decreased. This change in the plant community is likely a response to climate driven environmental change, but the temperature reconstructions are not thought to be wholly representative of the then climate.

The plant trait-based temperature reconstruction indicated a strong turnover in the vegetation classes from cooler-preferring arctic-alpine plants to warmer-preferring plants at the start of the Holocene (c. 11,500–8900 cal yr BP). There was a peak in the plant temperature requirement at c. 9000 cal yr BP, after which the values decreased slightly to c. 7780 cal yr BP. There were comparable trends between the plant trait-based temperature curve and the CHELSA TraCE21k July temperature (Pearson's correlation = −0.657, p value = 0.006, Supplementary Fig. 35) and NGRIP isotope (Pearson's correlation = −0.769, p value < 0.000, Supplementary Fig. 36) records.

4.2. Heathland formation and lake acidification during a wetter mid-Holocene (c. 7800 to 3300 cal yr BP, biota zones Dz4 and Cz5)

The mid-Holocene is generally considered to have a more stable climate, driven by weakened orbital forcing during northern hemisphere summers (Wanner et al., 2008), which had greater effect in high latitude regions (Balascio and Bradley, 2012). At Horntjernet, the sedimentological proxies indicate a more stable environment; with largely organic-rich lake sediment, and a lower K/Ti content suggesting a thicker soil profile and reduction in physical weathering in the local catchment (Arnaud et al., 2012). Relatively stable DCA axis 1 scores indicate lower turnover in the ecological communities.

4.2.1. Mixed birch-pine woodland with heathland taxa

On the landscape, the vegetation record was characterised by a mixed birch-pine woodland with heathland taxa, from c. 7900 to 3300 cal yr BP. *Betula* and *Pinus sylvestris* were the dominant tree/shrub taxa, with *Populus tremula*, *Sorbus aucuparia,* and *Juniperus communis* also present on the landscape. The dominant functional group was dwarf shrubs, with *Empetrum nigrum*, *Andromeda polifolia*, and *Vaccinium* species present, indicating a large presence of heath-type plants. Early development of heathland is observed in other regional records (Rijal et al., 2021; Seppä et al., 2002). The increase in heathland taxa suggests a wetter climate. The localised CHELSA TraCE21k precipitation reconstruction indicates an increase in precipitation from c. 8000 to 2000 cal yrs BP. The trait-based moisture requirement analysis indicated a plant community with mesic-moist to moist water requirements. At c. 5500 - 3300 cal yr BP, there was a decrease in taxa that prefer mesic, well-drained soils, including tree/shrub taxa *Sorbus aucuparia* and *Juniperus communis*, dwarf shrub *Vaccinium vitis idea*, and forbs *Melampyirum* cf. *pratense* and *Solidago* (Tyler et al., 2021). At c. 4800 to 4000 cal yr BP, there was an increase in bryophytes and vascular cryptogams, suggesting the region became increasingly wetter

throughout the mid-late Holocene. Alsos et al. (2022) and Salonen et al. (2024) also indicated plant communities with a higher moisture requirement during the mid-Holocene. The large presence of heathland taxa suggests the soil was more acidic. This is supported by the plant trait-based pH analysis, which indicated the plant community had an ecological preference for moderately acidic soils (pH 4.5–5.5). The soil acidification likely resulted from the establishment of *Pinus sylvestris* (which arrived on the landscape c. 8900 cal yr BP) altering the soil microbial ecosystem and lowering the soil pH (Arnold, 1992). It is likely that the combination of a wetter mid-Holocene and increased soil acidity caused lake acidification.

4.2.2. Lake acidification

The aquatic community experienced decreased taxonomic richness and diversity, likely due to acidification driven by an increase in effective moisture, change in catchment vegetation, and associated increase in humic acid inputs from the catchment (Il'yashuk et al., 2005). The aquatic plant community comprised two dominant species, eurytopic *Nannochloropsis granulata* and acid-tolerant *Menyanthes trifoliata*. The decrease in abundance and diversity of aquatic macrophytes is indicative of a lower water pH (Rørslett, 1991), and *Menyanthes trifoliata* has been shown to have a pH preference of 5.23–5.55 (Serafin et al., 2017). The chironomid community was dominated by one taxon, *Sergentia coracina*-type. While typically a cold stenotherm, *Sergentia coracina*-type is also acid tolerant (Antonsson et al., 2006; Il'yashuk and Il'yashuk, 2000; Olander et al., 1999) and found in humic/coloured lakes (Heiri, 2004; Korhola et al., 2002). In humic lakes, bottom waters are likely to be susceptible to anoxia due to reduced light penetration and photochemical oxidation of dissolved organic substances (Heiri, 2004). Anoxia, or lack of oxygen availability, has a direct influence on the composition and abundance of chironomids (Brodersen et al., 2004; Quinlan and Smol, 2001; Ursenbacher et al., 2020). The chironomid assemblage in zone Cz4 has a decreased taxonomic diversity, and *Sergentia coracina*-type can survive in moderate oxygen-depleted conditions (Quinlan and Smol, 2001), thus it is possible that Lake Horntjernet experienced increased anoxia at this time. Other chironomid taxa present in this zone are acid tolerant (*Psectrocladius sordidellus*-type (Luoto, 2011; Nazarova et al., 2017),), or indicative of nutrient-rich conditions (*Procladius* sp. (Langdon et al., 2006; Luoto, 2011) and *Tanytarsus glabrescens*-type (Heiri et al., 2011)). It is possible there was an increase in nutrient input into Horntjernet following long-term soil development and increased precipitation. However, if the change in water quality was driven by nutrient input, it is more likely that macrophyte abundance would have increased (Mjelde et al., 2023), whereas it decreased in Horntjernet. Revéret et al. (2023) found after c. 8000 cal yr BP, many aquatic macrophyte communities across Fennoscandian lakes indicated nutrient-poor water. Thus, it is more likely that lake acidification, and associated water quality changes, was the strongest driver of chironomid community composition during the mid-Holocene. Mid-Holocene lake acidification and its influence on chironomid assemblages has been recognised regionally, e.g. in Sweden (Antonsson et al., 2006) and the Kola Peninsula (Il'yashuk et al., 2005).

4.2.3. Cool mid-Holocene temperatures

The Horntjernet chironomid-inferred temperature reconstruction indicated cool temperatures (mean 11.3 °C, range 11.2–12.3 °C) between c. 7800 to 4700 cal yr BP. The regional proxy records (NGRIP and CHELSA TraCE21k) and local pollen-inferred and branched glycerol dialkyl glycerol tetraethers (brGDGTs) -inferred temperature reconstructions indicated a thermal maximum during this period (c. 7500 - 4000 cal yr BP, Otiniano et al., 2024; Shala et al., 2017). This indicates a de-coupling between the chironomid assemblages and temperature; changes in the catchment vegetation and increased precipitation had a stronger influence on the lake water quality than temperature, and thus the chironomid-inferred temperatures should be treated with caution during this part of the record. A similar mid-Holocene cooling was observed in chironomid-inferred temperature reconstructions from two Swedish boreal lakes, where the establishment of *Picea* in the catchment was associated with an increase in chironomids which are recognised as both cold-preferring and acid tolerant, and thus lowered the chironomid-inferred temperature reconstructions (Antonsson et al., 2006; Engels, 2021). The Lake Loitsana chironomid-inferred temperature reconstruction also indicated a cooler climate between c. 8700–6800 and 6000–4500 cal yr BP (Shala et al., 2017). The cooler reconstructed temperatures were related to large abundances of typically-cold stenotherms *Corynocera ambigua*–type and *Corynocera oliveri*–type. These taxa are not associated with acidic lakes, however *Corynocera oliveri*–type has been found in lakes with higher DOC concentrations (Gajewski et al., 2005; Medeiros and Quinlan, 2011), thus is it likely these chironomids were also responding to catchment-driven changes in the water quality.

Towards the mid-late Holocene boundary, c. 4600 - 3300 cal yr BP, the chironomid-inferred temperatures indicated warmer temperatures (mean 12.3 °C). This correlated with a small decrease in the abundance of *Sergentia coracina*-type, and an increase in more temperate taxa, such as *Psectrocladius sordidellus*-type, *Tanytarsus glabrescens*-type and *Zalutschia* type A (Brooks et al., 2007). This could be an indication of climate becoming the major driver on chironomid community again; regional records indicated warmer temperatures at this time, including the Barents Sea planktonic foraminifera sea surface temperature reconstruction (Hald et al., 2007) and Lake Loitsana pollen-inferred temperature record (Shala et al., 2017). The local CHELSA TraCE21k annual precipitation reconstruction and plant community indicates increasing precipitation this time. Engels and Cwynar (2011) indicated a threshold at 5–7 m lake water depth where changes in assemblage can be related to changes in water depth. Lake Horntjernet falls within this depth range; however, the biological proxies do not indicate clear evidence of changing lake depth; macrophytes do not change in abundance and there are increases and decreases in both littoral and profundal chironomid taxa. It is possible this change in chironomid community is associated with temperature; warmer temperatures were also recorded in the Lake Loitsana chironomid-inferred temperature record from c. 4500 cal yr BP (Shala et al., 2017). Shala et al. (2017) attribute this warming trend to increased abundances of *Cladotanytarsus mancus*-type and *Tanytarsus mendax*-type, which are typically warm-preferring taxa (Eggermont and Heiri, 2012), but are also found in shallow waters and nutrient-rich conditions (Luoto, 2011). Other records suggest maximum temperatures occurred earlier in northern Fennoscandia, e.g. c. 8000 to 6500 cal yr BP (Sejrup et al., 2016) or c. 9000–7000 to 5000 cal yr BP (Väliranta et al., 2015). This demonstrates that a combination of drivers was likely driving chironomid assemblage change during the mid-to late Holocene.

The plant-inferred and trait-based temperature reconstructions at Horntjernet during the mid-Holocene indicated overall stability, with a slight cooling. The plant-inferred temperatures were approx. 0.6 °C cooler (range 11.1–11.6 °C) than the temperatures in the early Holocene, while the trait-based temperature reconstruction suggested a slight decrease in the proportion of temperate taxa in the environment. The stability in the trait-based temperature reconstruction is likely due to the relatively even spread of taxa across the different temperature optimum classes (Supplementary Fig. 22). The stability in the plant-inferred temperature reconstruction is likely due to the dominance of *Pinus sylvestris*, *Vaccinium uliginosum,* and *Menyanthes trifoliata*, which were detected in all 8 repeats in every sample within Dz4 (Supplementary Fig. 15). These plants have mean temperature minima of 12.9, 9.5, and 12.6 °C respectively. *Vaccinium microcarpum* was also present in all samples, with a mean temperature minimum of 9.9 °C. None of the plant species used in the temperature reconstruction for Dz4 had mean temperature minima greater than 13.4 °C, and the 7 plant species present in every sample had mean temperature minima of 9.5–12.9 °C (Supplementary Fig. 17). In comparison to other records, the plant-inferred temperatures were cooler (range 11.1–11.6 °C); the

CHELSA TraCE21k July temperature reconstruction indicated temperatures between 14.1 and 17.4 °C, and published pollen-inferred temperatures indicate temperatures of approx. 11–14 °C in northern Norway (Bjune et al., 2004) and approx. 13–15 °C in northern Finland (Shala et al., 2017). Thus, the plant-inferred temperature reconstruction was limited by the taxa identified to species level and their mean temperature minima in the CHELSA TraCE21k database (Karger et al., 2017).

4.3. Ecological diversity and cooling during the late Holocene (c. 3300 cal yr BP to present, biota zones Dz5 and Cz5-6)

In the late Holocene, the sediment minerogenic content remained low and organic content remained high. At c. 1000 cal yr BP, there was an increase in sediment accumulation rate, and decrease in organic content, Ca/Ti and Si/Ti. Decreases in Ca/Ti and Si/Ti suggest a decrease in detrital input (Boës et al., 2011). There was a turnover in the plant and chironomid assemblages at this time, recognised by changes in the DCA axis 1 scores.

4.3.1. Diverse woodland and heathland vegetation communities

The vegetation record was relatively stable with a continuation of mixed birch-pine woodland and heathland taxa. *Populus tremula* and *Juniperus communis* were present throughout the zone, with *Alnus incana* present until c. 2000 cal yr BP, and *Sorbus aucuparia* appearing in the two most recent samples. Heathland taxa continued to dominate the dwarf shrub community, with *Calluna vulgaris* arriving on the landscape at c. 2600 cal yr BP. Forb *Drosera anglica* also appeared in the record at c. 2600 cal yr BP. *Calluna vulgaris* and *Drosera anglica* grow in open, non-forested habitats and ombrotrophic mires, suggesting the climate was cooler and wetter. Other studies also showed expansion of mires and heath vegetation regionally during the late Holocene (Bjune et al., 2004; Seppä, 1998; Sjögren and Damm, 2019). The alpine meadow plant *Rhododendron lapponicum,* requiring cool, moist growing conditions with a long snow-cover, appeared at c. 1200 cal yr BP. In the last 300 years, forb and grass taxa re-appeared, such as *Rumex*, *Carex*, *Avenella flexuosa* and *Phragmites australis*, suggesting a more open environment. Current vegetation around Lake Horntjernet consists of pine forest with scattered birch (*Betula pubescence*), shrubs (*Betula nana*, *Rhododendron tomentosum*) and mire. *Rumex* and *Solidago*, which can be associated with minor anthropogenic activity (Räsänen, 2001), were present in the most recent sample (c. 1980 CE). It is likely that there was some cutting of pine trees as it is recognised as a valuable timber in the region, and that this may have created more open space, allowing for the expansion of forbs and grasses.

4.3.2. Increased lake productivity and diversity

The aquatic plant community increased in diversity, with the appearance of *Utricularia*, and re-appearance of *Spaganium* and *Stuckenia vaginata*, suggesting an increase in the water pH (Mjelde et al., 2023). The localised CHELSA TraCE21k precipitation reconstruction indicates a change in the precipitation regime at this time, with a switch to more precipitation falling between September and May (Supplementary Fig. 5). Higher winter precipitation can reduce the amount of DOC washed into lakes in the warmer months, thus increasing the water pH (Tiwari et al., 2018). In the chironomid record, *Sergentia coracina*-type notably decreased in abundance and was replaced with *Tanytarsus glabrescens*-type (thermophilic, associated with productive, nutrient rich lakes, Brooks and Heiri, 2013; Perret-Gentil et al., 2024), *Parakiefferiella bathophila*-type (associated with warmer, more eutrophic lakes, Brooks, 2006; Gouw-Bouman et al., 2019) and *Psectrocladius sordidellus*-type (temperate lakes, macrophytes, shallow waters, acidophilic, Langdon et al., 2010; Luoto and Salonen, 2010; Nazarova et al., 2017). These in-lakes changes in community suggest the lake was less acidic and more nutrient rich. In the uppermost zone (c. 800 cal yr BP to present), *Chironomus anthracinus*-type, which often appears after environmental change (Brooks, 2006; Brooks et al., 2007), re-appeared indicating disturbance within the catchment, possibly associated with deforestation and opening of the environment.

4.3.3. Late Holocene cooling

The NGRIP oxygen isotope record (Wolff et al., 2010) and CHELSA TraCE21k July temperature reconstruction (Karger et al., 2023) indicate late Holocene cooling. Cooling is also observed in pollen-inferred July temperature reconstructions from the Fennoscandian treeline (Seppä and Birks, 2001) and northern Norway (Bjune et al., 2004). The Horntjernet chironomid-inferred temperature reconstruction indicated a general cooling trend from c. 3300 cal yr BP to present, in agreement with the NGRIP and CHELSA TraCE21k curves (Pearson's correlation indicates moderate correlations, Supplementary Figs. 29 and 30). Other regional chironomid-inferred temperature records also indicate late Holocene cooling in Finland (Luoto et al., 2014b; Sarmaja-Korjonen et al., 2006), Sweden (Antonsson et al., 2006), and the Kola Peninsula (Il'yashuk et al., 2013). The Lake Loitsana chironomid-inferred temperature record shows increased late Holocene temperatures (Shala et al., 2017), however, Shala et al. (2017) interpret this as an artefact of local factors including shallowing-related eutrophication. The Horntjernet chironomid-inferred temperature record does not indicate clear temperature changes in association with the MCA (c. 950 to 1250 CE, Mann et al., 2009) or LIA (c. 1400 to 1700 CE, Mann et al., 2009). A brief cold oscillation was identified at c. 1800 cal yr BP in a chironomid-inferred temperature reconstruction from NW Finland (Korhola et al., 2002), however no warming trend was identified in this record. Other regional chironomid-inferred temperature records do not identify temperature changes in association with these late Holocene climate events, likely due to the low temporal resolution of the sediment profiles (Antonsson et al., 2006; Engels, 2021; Il'yashuk et al., 2013; Luoto et al., 2014b; Sarmaja-Korjonen et al., 2006). The most recent chironomid-inferred temperature was approx. 12.0 °C at 240 cal yr BP (c. 1780 CE), within the bounds of the LIA, which was dated to the c. mid-1800s CE (c. 250 - 150 cal yr BP) in Northern Norway (Leigh et al., 2020; Nesje, 2009). The present-day mean July temperature at Lake Horntjernet is 13.8 °C (1993–2019 CE, Pasvik National Nature Reserve, 2023), 1.8 °C warmer than the most recent chironomid-inferred temperature.

The Horntjernet plant-inferred temperature record ranged between 11.8 and 11.1 °C in the late Holocene, approx. 2–2.7 °C cooler than present. The trait-based plant temperature reconstruction was variable in the late Holocene, with no clear cooling trend. Thus, not fitting with the trends recorded in other regional records, including the CHELSA TraCE21k July temperature reconstruction (Karger et al., 2023), and the NGRIP oxygen isotope record (Wolff et al., 2010). Both the plant-inferred and trait-based reconstructions indicated a slight cooling at c. 1200 to 570 cal yr BP (750–1680 CE) and warming at c. 300 to 30 cal yr BP (1650–1920 CE). This is the opposite trend to expected in relation to the MCA (c. 950 to 1250 CE) and LIA (c. 1400 to 1700 CE) (M. E. Mann et al., 2009; Wanner et al., 2008). Other plant-inferred temperature reconstructions from northern Fennoscandia indicate late Holocene cooling, with MCA and LIA oscillations (Bjune et al., 2004; Seppä and Birks, 2001). The most recent (c. −30 cal yr BP or c. 1980 CE) plant sample indicated cooler temperatures, the plant-inferred temperature was 11.3 °C, 2.5 °C lower than the local average 13.8 °C (from 1993 to 2019 CE), while the trait-based temperature reconstruction indicated a greater proportion of cool-preferring arctic/alpine plants. This is likely driven by the expansion of forbs and grasses following localised deforestation. The most recent value in the CHELSA TraCE21k July temperature reconstruction is 13.6 °C, comparable to modern temperatures.

4.4. Limitations of reconstructing Holocene temperature change

Multiproxy analyses offer greater insight into past climate and environmental change, however, proxy methods represent different

parts of a landscape or ecosystem, and thus reflect different aspects of climate or environment change, or can be influenced by other variables (Antonsson et al., 2006). Disassociating trends driven by regional or local drivers of proxy variation is important for interpreting palaeoecological data. At Horntjernet, plant community composition can be broadly explained by relatively well-known bioclimatic relationships. There is widespread evidence across Norway and Fennoscandia to indicate Holocene environmental development (Alsos et al., 2022; Rijal et al., 2021). Temperature requirement had a large influence on the arrival time of taxa following the deglaciation of the Scandinavian Ice Sheet, with taxa associated with cooler temperatures generally arriving earlier. This trend is observed regionally (Alsos et al., 2022). Comparison between the plant community turnover (DCA axis 1 scores) and the independent (NGRIP/CHELSA TraCE21k) climate records (Supplementary Figs. 26–27), suggests some lag in the plant development. Providing there is confidence in the age-model(s), this suggests there is a delayed migrational response of plants to abrupt, large-scale climatic events, due to the time required for plants to grow, reproduce and produce biomass which can be preserved in the record (e.g. *sed*aDNA and pollen) (Seppä et al., 2004). Other limits on early Holocene Arctic tree expansion can include growing season length and moisture availability (Mann et al., 2002; Miller et al., 2008). In Northern Fennoscandia, it took millennia for the current regional flora to arrive after deglaciation, and with some cold adapted species not arriving until the late Holocene (Alsos et al., 2022). On a local scale, the Lake Horntjernet water quality and chironomid assemblages were strongly influenced by catchment development; indicated by the strong relationship between the chironomid community turnover and organic matter content and plant community turnover (Supplementary Fig. 24). This close inter-connectedness has been observed in other studies (Cardille et al., 2007; Porinchu and Cwynar, 2000) and is likely due to the physiology of the lake, such as the relatively small size (Staehr et al., 2012) and shallowness (Lim et al., 2005; Medeiros et al., 2012). In this record, it is likely that lake acidification influenced the chironomid record, which at least partially confounded an accurate climatic reconstruction (Heiri and Lotter, 2003; Il'yashuk et al., 2005; Velle et al., 2010).

Biogeographic constraints, such as oceans or mountain ranges, can be key factors limiting chironomid dispersal to new habitats across broad high latitude regions (Medeiros et al., 2021). Horntjernet is located in the north of Fennoscandia and 70 km up a major fault-controlled fjord system, thus there is a large expanse of land around Horntjernet, combined with the early deglaciation of the Fennoscandian ice sheet (Hughes et al., 2016). It is likely that multiple terrestrial corridors of dispersal existed during the early Holocene, promoting rapid chironomid dispersal at the end of the last glaciation. This is evident in the rapid turnover in the chironomid community during the early Holocene. The taxon with the greatest influence on the temperature reconstruction was *Sergentia coracina*-type. Medeiros et al. (2021) considered *Sergentia coracina*-type common across high latitude regions. It is possible the temperature reconstruction calculation method (WA-PLS) placed too much emphasis on *Sergentia coracina*-type and its typically cold climatic preferences. There is a known tendency for WA-PLS to calculate reconstructions focused on the centre of the climatic ranges within the calibration dataset, potentially biasing the reconstructed past temperatures. To account for this, Liu et al. (2020) formulated a tolerance-weighted WA-PLS, which placed more emphasis on taxa with narrower tolerances. However, this is unlikely to have removed the cooling effect of *Sergentia coracina*-type on the temperature reconstruction, due to the large numbers of *Sergentia coracina*-type present. Additionally, the chironomid record fits within the expected temperature trends based on other regional chironomid records. This supports the idea of local or in-lake environmental drivers having significant influence on the chironomid assemblages.

The calculated values of the *sed*aDNA plant-inferred temperature reconstruction are not representative of realistic climatic change in the Horntjernet record. This is likely due to limitations in the number of taxa identified to species level and the persistence of species with wide and varied thermal ranges causing a regression to the mean. Taxa which were identified to species level and had repeats of 8 had a strong control on the calculated temperatures. Horntjernet was not the most species-rich site analysed for plant *sed*aDNA across the region (Rijal et al., 2021). Thus, it is possible that a lake with a greater species richness on the treeline (Garcés-Pastor et al., 2022), or perhaps a combined multi-lake analysis, such as in Alsos et al. (2022) might have produced a more realistic temperature reconstruction. It is also possible that the usage of mean minima temperatures prevented a greater range of calculated temperatures; it is noted that the CHELSA TraCE21k July temperature reconstruction produced a large range of reconstructed temperatures. Large-scale climatic simulations, such as the CHELSA TraCE21k July temperature reconstruction, are useful for understanding large-scale patterns of climate change across space and time, however, they are perhaps not as reliable for providing absolute values, e.g. here an approx. 8 °C magnitude of temperature change was calculated in the CHELSA TraCE21k July temperature reconstruction during the early Holocene, compared to magnitudes of approx. 3 °C of change in regional pollen-inferred and chironomid-inferred temperature reconstructions. Data on small-scale changing climatic conditions, such as those presented here, can increase understanding of localised climate impacts on biodiversity and ecosystem functioning (Zellweger et al., 2024). Thus, here we present one of the first attempts at using *sed*aDNA to reconstruct temperatures (see Elliott et al. (2023) for another), which suggests that new approaches, such as trait-based analyses, are required to produce robust temperature reconstructions.

5. Conclusions

Lake Horntjernet developed soon after deglaciation and before c. 11,500 cal yr BP. The sediments provide valuable information about broad-scale environmental change; rapid vegetation development with early arrival of trees and lake acidification following the establishment of pine forest and heathlands. The lake is strongly affected by developments in the catchment, which is reflected in the chironomid community. Due to this, the chironomid community produces a temperature reconstruction with mixed reliability. The temperature record is partly confounded by local effects during the more climatically stable mid-Holocene, while the trends in the early and late Holocene are more comparable to expected regional patterns. The attempt to use plant *sed*aDNA data for climatic reconstruction using mean minimum July temperatures from the CHELSA plant observational (biogeographical) database does not produce convincing temperature trends. This is likely due to the early development of macrophyte communities and persistence of taxa with varied thermal ranges after the development of the boreal forest, suggesting that the selection of weighted ranges or biome-specific calibration sets may be required to obtain more accurate temperature reconstructions. A trait-based optimum approach did provide a Holocene trend similar to that of CHELSA TraCE21k and NGRIP reconstructions. Thus, here we indicate the value of combined sedimentary, *sed*aDNA and chironomid proxies for deciphering the complex response of local boreal ecosystems to climate change.

Author contributions

RJM, IGA, PGL discussed the research conceptualization, all co-authors discussed the research outcomes. IGA and DPR organised the field campaign. RJM and DPR were part of the field team. AGB provided uplift correction, archaeological and regional knowledge. IGA provided botanical taxonomic and regional knowledge. RJM processed, identified, and interpreted the chironomid samples at the University of Southampton, with guidance from PGL. PDH and RJM produced the age model and accumulation rate data. Plant samples were processed (DNA preparation, identification, and interpretation) by IGA, DPR, PDH at UiT

- The Arctic University of Norway. Plant temperature ranges and CHELSA TraCE21k reconstructions were provided by DHK. Temperature reconstructions were calculated by RJM. Plant Trait Analysis was run by DPR. Other statistical analyses and graphics were produced by RJM. RJM wrote the first manuscript draft, on which all co-authors commented.

Funding

DPR, PDH, and IGA were funded by the Research Council of Norway (grant 250963/F20, "ECOGEN"). RJM was supported by a Ph.D. studentship awarded by the UK National Environmental Research Council (grant no. NE/L002531/1).

Declaration of Competing Interest

The authors have no conflicts or declarations of interest. No AI has been used in the creation of this manuscript.

Acknowledgments

We thank Iva Pitelkova for conducting the LOI analysis, Enrique Tejero Caballo and Karina Monsen for conducting the XRF scanning and high-resolution imagery, Francisco Javier Ancin Murguzur for assistance with coring and fieldwork, and Youri Lammers for help with bioinformatic processing. Thanks to Charlotte Clarke and Iva Pitelkova for sub-sampling sediment for the chironomid analysis and Thierry Fonville for guidance on producing chironomid temperature reconstructions in R. Thank you to Maarten van Hardenbroek and Steve Brooks for informal chironomid discussions. Thanks to Dr Marianne Skandfer for her archaeological information.

Appendix A. Supplementary data

Supplementary data to this article can be found online at https://doi.org/10.1016/j.quascirev.2024.109045.

Data availability

Data is either shared with this manuscript as a Supplementary Dataset, or already publicly available.

References

Aarnes, I., Bjune, A.E., Birks, H.H., Balascio, N.L., Bakke, J., Blaauw, M., 2012. Vegetation responses to rapid climatic changes during the last deglaciation 13,500-8,000 years ago on southwest Andøya, arctic Norway. Veg. Hist. Archaeobotany 21 (1), 17–35. https://doi.org/10.1007/s00334-011-0320-4.

Alsos, I.G., Rijal, D.P., Ehrich, D., Karger, D.N., Yoccoz, N.G., Heintzman, P.D., Brown, A. G., Lammers, Y., Pellissier, L., Alm, T., Bråthen, K.A., Coissac, E., Merkel, M.K.F., Alberti, A., Denoeud, F., Bakke, J., 2022. Postglacial species arrival and diversity buildup of northern ecosystems took millennia. Sci. Adv. 8 (39), eabo7434. https://doi.org/10.1126/sciadv.abo7434.

Alsos, I.G., Sjögren, P., Edwards, M.E., Landvik, J.Y., Gielly, L., Forwick, M., Coissac, E., Brown, A.G., Jakobsen, L.V., Føreid, M.K., Pedersen, M.W., 2016. Sedimentary ancient DNA from Lake Skartjørna, Svalbard: assessing the resilience of arctic flora to Holocene climate change. Holocene 26 (4), 627–642. https://doi.org/10.1177/0959683615612563.

Antonsson, K., Brooks, S.J., Seppä, H., Telford, R.J., Birks, H.J.B., 2006. Quantitative palaeotemperature records inferred from fossil pollen and chironomid assemblages from Lake Gilltjärnen, northern central Sweden. J. Quat. Sci. 21 (8), 831–841. https://doi.org/10.1002/jqs.1004.

Arnaud, F., Révillon, S., Debret, M., Revel, M., Chapron, E., Jacob, J., Giguet-Covex, C., Poulenard, J., Magny, M., 2012. Lake Bourget regional erosion patterns reconstruction reveals Holocene NW European Alps soil evolution and paleohydrology. Quat. Sci. Rev. 51, 81–92. https://doi.org/10.1016/j.quascirev.2012.07.025.

Arnold, G., 1992. Soil acidification as caused by the nitrogen uptake pattern of Scots pine (*Pinus sylvestris*). Plant Soil 142 (1), 41–51. https://doi.org/10.1007/BF00010173.

Artaxo, P., Hansson, H.C., Andreae, M.O., Bäck, J., Alves, E.G., Barbosa, H.M.J., Bender, F., Bourtsoukidis, E., Carbone, S., Chi, J., Decesari, S., Després, V.R., Ditas, F., Ezhova, E., Fuzzi, S., Hasselquist, N.J., Heintzenberg, J., Holanda, B.A., Guenther, A., et al., 2022. Tropical and boreal forest - atmosphere interactions: a review. Tellus Ser. B Chem. Phys. Meteorol. 74 (1), 24–163. https://doi.org/10.16993/tellusb.34.

Axford, Y., Levy, L.B., Kelly, M.A., Francis, D.R., Hall, B.L., Langdon, P.G., Axford, T.V.L., Levy, Y., Kelly, L.B., Francis, M.A., Langdon, D.R., Lowell, P.G., 2017. Timing and magnitude of early to middle Holocene warming in East Greenland inferred from chironomids. Boreas 46 (4), 678–687. https://doi.org/10.1111/bor.12247.

Balascio, N.L., Bradley, R.S., 2012. Evaluating Holocene climate change in northern Norway using sediment records from two contrasting lake systems. J. Paleolimnol. 48 (1), 259–273. https://doi.org/10.1007/s10933-012-9604-7.

Barley, E.M., Walker, I.R., Kurek, J., Cwynar, L.C., Mathewes, R.W., Gajewski, K., Finney, B.P., 2006. A northwest North American training set: distribution of freshwater midges in relation to air temperature and lake depth. J. Paleolimnol. 36 (3), 295–314. https://doi.org/10.1007/s10933-006-0014-6.

Belle, S., Johnson, R.K., 2024. Acidification of freshwater lakes in Scandinavia: impacts and recovery of chironomid communities under accelerating environmental changes. Hydrobiologia 851 (3), 585–600. https://doi.org/10.1007/s10750-023-05346-9.

Bennion, H., Sayer, C.D., Clarke, S.J., Davidson, T.A., Rose, N.L., Goldsmith, B., Rawcliffe, R., Burgess, A., Clarke, G., Turner, S., Wiik, E., 2018. Sedimentary macrofossil records reveal ecological change in English lakes: implications for conservation. J. Paleolimnol. 60 (2), 329–348. https://doi.org/10.1007/s10933-017-9941-7.

Birks, H.H., 2003. The importance of plant macrofossils in the reconstruction of Lateglacial vegetation and climate: examples from Scotland, western Norway, and Minnesota, USA. Quat. Sci. Rev. 22 (5–7), 453–473. https://doi.org/10.1016/S0277-3791(02)00248-2.

Birks, H.H., 2015. South to north: contrasting late-glacial and early-Holocene climate changes and vegetation responses between south and north Norway. Holocene 25 (1), 37–52. https://doi.org/10.1177/0959683614556375.

Birks, H.H., Battarbee, R.W., Birks, H.J.B., Bradshaw, E.G., Brooks, S.J., Duigan, C.A., Jones, V.J., Lemdahl, G., Peglar, S.M., Solem, J.O., Solhøy, I.W., Solhøy, T., Stalsberg, M.K., 2000. The development of the aquatic ecosystem at Kråkenes Lake, western Norway, during the late-glacial and early-Holocene - a synthesis. J. Paleolimnol. 23 (1), 91–114. https://doi.org/10.1023/A:1008079725596.

Birks, H.H., Birks, H.J.B., 2000. Future uses of pollen analysis must include plant macrofossils. J. Biogeogr. 27 (1), 31–35. https://doi.org/10.1046/j.1365-2699.2000.00375.x.

Birks, H.H., Birks, H.J.B., 2006. Multi-proxy studies in palaeolimnology. Veg. Hist. Archaeobotany 15, 235–251. https://doi.org/10.1007/s00334-006-0066-6.

Birks, H.H., Jones, V.J., Brooks, S.J., Birks, H.J.B., Telford, R.J., Juggins, S., Peglar, S.M., 2012. From cold to cool in northernmost Norway: lateglacial and early Holocene multi-proxy environmental and climate reconstructions from Jansvatnet, Hammerfest. Quat. Sci. Rev. 33, 100–120. https://doi.org/10.1016/j.quascirev.2011.11.013.

Birks, H.J.B., Birks, H.H., 2008. Biological responses to rapid climate change at the Younger Dryas-Holocene transition at Kråkenes, western Norway. Holocene 18 (1), 19–30. https://doi.org/10.1177/0959683607085572.

Bjorkman, A.D., García Criado, M., Myers-Smith, I.H., Ravolainen, V., Jónsdóttir, I.S., Westergaard, K.B., Lawler, J.P., Aronsson, M., Bennett, B., Gardfjell, H., Heiðmarsson, S., Stewart, L., Normand, S., 2020. Status and trends in Arctic vegetation: evidence from experimental warming and long-term monitoring. Ambio 49 (3), 678–692. https://doi.org/10.1007/s13280-019-01161-6.

Bjune, A., Birks, H.J.B., Seppä, H., 2004. Holocene vegetation and climate history on a continental-oceanic transect in northern Fennoscandia based on pollen and plant macrofossils. Boreas 33 (3), 211–223. https://doi.org/10.1080/03009480410001244.

Bjune, A.E., Birks, H.J.B., Peglar, S.M., Odland, A., 2010. Developing a modern pollen-climate calibration data set for Norway. Boreas 39 (4), 674–688. https://doi.org/10.1111/j.1502-3885.2010.00158.x.

Blaauw, M., Christen, J.A., 2011. Flexible paleoclimate age-depth models using an autoregressive gamma process. Bayesian Analysis 6 (3), 457–474. https://doi.org/10.1214/11-ba618.

Boës, X., Rydberg, J., Martinez-Cortizas, A., Bindler, R., Renberg, I., 2011. Evaluation of conservative lithogenic elements (Ti, Zr, Al, and Rb) to study anthropogenic element enrichments in lake sediments. J. Paleolimnol. 46 (1), 75–87. https://doi.org/10.1007/s10933-011-9515-z.

Bonan, G.B., Pollard, D., Thompson, S.L., 1992. Effects of boreal forest vegetation on global climate. Nature 359 (6397), 716–718. https://doi.org/10.1038/359716a0.

Boyle, J., Chiverrell, R., Plater, A., Thrasher, I., Bradshaw, E., Birks, H., Birks, J., 2013. Soil mineral depletion drives early Holocene lake acidification. Geology 41 (4), 415–418. https://doi.org/10.1130/G33907, 1.

Bradshaw, E.G., Rasmussen, P., Odgaard, B.V., 2005. Mid- to late-Holocene land-use change and lake development at Dallund Sø, Denmark: synthesis of multiproxy data, linking land and lake. Holocene 15 (8), 1152–1162. https://doi.org/10.1191/0959683605hl887rp.

Brodersen, K.P., Odgaard, B.V., Vestergaard, O., Anderson, N.J., 2001. Chironomid stratigraphy in the shallow and eutrophic Lake Søbygaard, Denmark: chironomid-macrophyte co-occurrence. Freshw. Biol. 46 (2), 253–267. https://doi.org/10.1046/j.1365-2427.2001.00652.x.

Brodersen, K.P., Pedersen, O., Lindegaard, C., Hamburger, K., 2004. Chironomids (Diptera) and oxy-regulatory capacity: an experimental approach to paleolimnological interpretation. Limnol. Oceanogr. 49 (5), 1549–1559. https://doi.org/10.4319/lo.2004.49.5.1549.

Brooks, S.J., 2006. Fossil midges (Diptera: chironomidae) as palaeoclimatic indicators for the Eurasian region. Quat. Sci. Rev. 25 (15–16), 1894–1910. https://doi.org/10.1016/j.quascirev.2005.03.021.

Brooks, S.J., Axford, Y., Heiri, O., Langdon, P.G., Larocque-Tobler, I., 2012a. Chironomids can be reliable proxies for Holocene temperatures. A comment on Velle et al. (2010). Holocene 22 (12), 1495–1500. https://doi.org/10.1177/0959683612449757.

Brooks, S.J., Birks, H.J.B., 2000. Chironomid-inferred late-glacial and early-Holocene mean July air temperatures for Kråkenes Lake, western Norway. J. Paleolimnol. 23, 77–89. https://doi.org/10.1023/A:1008044211484.

Brooks, S.J., Birks, H.J.B., 2004. The dynamics of Chironomidae (Insecta: Diptera) assemblages in response to environmental change during the past 700 years on Svalbard. J. Paleolimnol. 31, 483–498. https://doi.org/10.1023/B:JOPL.0000022547.98465.d3.

Brooks, S.J., Davies, K.L., Mather, K.A., Matthews, I.P., Lowe, J.J., 2016. Chironomid-inferred summer temperatures for the last glacial-interglacial transition from a lake sediment sequence in muir Park reservoir, west-central scotland. J. Quat. Sci. 31 (3), 214–224. https://doi.org/10.1002/jqs.2860.

Brooks, S.J., Heiri, O., 2013. Response of chironomid assemblages to environmental change during the early Late-glacial at Gerzensee, Switzerland. Palaeogeogr. Palaeoclimatol. Palaeoecol. 391, 90–98. https://doi.org/10.1016/j.palaeo.2012.10.022.

Brooks, S.J., Langdon, P.G., Heiri, O., 2007. The identification and use of palaearctic chironomidae larvae in palaeoecology. QRA Techical Guide No. 10. Quaternary Research Association, London, p. 276.

Brooks, S.J., Matthews, I.P., Birks, H.H., Birks, H.J.B., 2012b. High resolution Lateglacial and early-Holocene summer air temperature records from Scotland inferred from chironomid assemblages. Quat. Sci. Rev. 41, 67–82. https://doi.org/10.1016/j.quascirev.2012.03.007.

Brown, T., Rijal, D.P., Heintzman, P.D., Clarke, C.L., Blankholm, H.P., Høeg, H.I., Lammers, Y., Bråthen, K.A., Edwards, M., Alsos, I.G., 2022. Paleoeconomy more than demography determined prehistoric human impact in Arctic Norway. PNAS Nexus 1 (5), pgac209. https://doi.org/10.1093/pnasnexus/pgac209.

Brundin, L., 1949. Chironomiden und andere Bodentiere der südschwedischen Urgebirgsseen: ein Beitrag zur Kenntnis der bodenfaunistischen Charakterzüge schwedischer oligotropher Seen. Carl Bloms Boktr play.google.com/store/books/details?id=C5ocAQAAMAAJ.

Capron, E., Govin, A., Stone, E.J., Masson-Delmotte, V., Mulitza, S., Otto-Bliesner, B., Rasmussen, T.L., Sime, L.C., Waelbroeck, C., Wolff, E.W., 2014. Temporal and spatial structure of multi-millennial temperature changes at high latitudes during the Last interglacial. Quat. Sci. Rev. 103, 116–133. https://doi.org/10.1016/j.quascirev.2014.08.018.

Cardille, J.A., Carpenter, S.R., Coe, M.T., Foley, J.A., Hanson, P.C., Turner, M.G., Vano, J. A., 2007. Carbon and water cycling in lake-rich landscape connections, lake hydrology, and biogeochemistry. J. Geophys. Res.: Biogeosciences 112, G02031. https://doi.org/10.1029/2006JG000200.

Clarke, C.L., Alsos, I.G., Edwards, M.E., Paus, A., Gielly, L., Haflidason, H., Mangerud, J., Regnéll, C., Hughes, P.D.M., Svendsen, J.I., Bjune, A.E., 2020. A 24,000-year ancient DNA and pollen record from the Polar Urals reveals temporal dynamics of arctic and boreal plant communities. Quat. Sci. Rev. 247, 106564. https://doi.org/10.1016/j.quascirev.2020.106564.

Clarke, C.L., Edwards, M.E., Brown, A.G., Gielly, L., Lammers, Y., Heintzman, P.D., Ancin-Murguzur, F.J., Bråthen, K.A., Goslar, T., Alsos, I.G., 2019. Holocene floristic diversity and richness in northeast Norway revealed by sedimentary ancient DNA (sedaDNA) and pollen. Boreas 48 (2), 299–316. https://doi.org/10.1111/bor.12357.

Cohen, A.S., 2003. Paleolimnology: the History and Evolution of Lake Systems. Oxford university press, New York, p. 528.

Eggermont, H., Heiri, O., 2012. The chironomid-temperature relationship: expression in nature and palaeoenvironmental implications. Biol. Rev. 87 (2), 430–456. https://doi.org/10.1111/j.1469-185X.2011.00206.x.

Elliott, L.D., Rijal, D.P., Brown, A.G., Bakke, J., Topstad, L., Heintzman, P.D., Alsos, I.G., 2023. Sedimentary ancient DNA reveals local vegetation changes driven by glacial activity and climate. Quaternary 6 (1), 7. https://doi.org/10.3390/quat6010007.

Elmendorf, S.C., Henry, G.H., Hollister, R.D., Björk, R.G., Boulanger-Lapointe, N., Cooper, E.J., Cornelissen, J.H., Day, T.A., Dorrepaal, E., Elumeeva, T.G., Gill, M., 2012. Plot-scale evidence of tundra vegetation change and links to recent summer warming. Nat. Clim. Change 2 (6), 453–457. https://doi.org/10.1038/nclimate1465.

Elven, R., Murray, D., Razzhivin, V., Yurtsev, B.A., 2011. Annotated Checklist of the Panarctic Flora (PAF): Vascular Plants. Natural History Museum, University of Oslo (2011). https://www.semanticscholar.org/paper/719689be41841bf81cfda0310e5e42f840a86a22. (Accessed 28 January 2023).

Engels, S., 2021. The influence of Holocene forest dynamics on the chironomid fauna of a boreal lake (Flocktjärn, northeast Sweden). Boreas 50 (2), 519–534. https://doi.org/10.1111/bor.12497.

Engels, S., Cwynar, L.C., 2011. Changes in fossil chironomid remains along a depth gradient: evidence for common faunal thresholds within lakes. Hydrobiologia 665 (1), 15–38. https://doi.org/10.1007/s10750-011-0601-z.

European Environment Agency, 2016. Biogeographical regions, Europe 2016, version 1. EEA geospatial data catalogue. https://www.eea.europa.eu/en/analysis/maps-and-charts/biogeographical-regions-in-europe-2. (Accessed 6 May 2021).

Gajewski, K., Bouchard, G., Wilson, S.E., Kurek, J., Cwynar, L.C., 2005. Distribution of Chironomidae (Insecta: Diptera) head capsules in recent sediments of Canadian Arctic lakes. Hydrobiologia 549 (1), 131–143. https://doi.org/10.1007/s10750-005-5444-z.

Garcés-Pastor, S., Coissac, E., Lavergne, S., Schwörer, C., Theurillat, J.P., Heintzman, P. D., Wangensteen, O.S., Tinner, W., Rey, F., Heer, M., Rutzer, A., Walsh, K., Lammers, Y., Brown, A.G., Goslar, T., Rijal, D.P., Karger, D.N., Pellissier, L., Pouchon, C., et al., 2022. High resolution ancient sedimentary DNA shows that alpine plant diversity is associated with human land use and climate change. Nat. Commun. 13 (1), 6559. https://doi.org/10.1038/s41467-022-34010-4.

Gouw-Bouman, M.T.I.J., van Asch, N., Engels, S., Hoek, W.Z., 2019. Late Holocene ecological shifts and chironomid-inferred summer temperature changes reconstructed from Lake Uddelermeer, The Netherlands. Palaeogeogr. Palaeoclimatol. Palaeoecol. 535, 109366. https://doi.org/10.1016/j.palaeo.2019.109366.

Hald, M., Andersson, C., Ebbesen, H., Jansen, E., Klitgaard-Kristensen, D., Risebrobakken, B., Salomonsen, G.R., Sarnthein, M., Sejrup, H.P., Telford, R.J., 2007. Variations in temperature and extent of atlantic water in the northern north atlantic during the Holocene. Quat. Sci. Rev. 26 (25–28), 3423–3440. https://doi.org/10.1016/j.quascirev.2007.10.005.

Heiri, O., 2004. Within-lake variability of subfossil chironomid assemblages in shallow Norwegian lakes. J. Paleolimnol. 32, 67–84.

Heiri, O., Brooks, S.J., Birks, H.J.B., Lotter, A.F., 2011. A 274-lake calibration data-set and inference model for chironomid-based summer air temperature reconstruction in Europe. Quat. Sci. Rev. 30 (23–24), 3445–3456. https://doi.org/10.1016/j.quascirev.2011.09.006.

Heiri, O., Lotter, A.F., 2001. Effect of low count sums on quantitative environmental reconstructions: an example using subfossil chironomids. J. Paleolimnol. 26, 343–350.

Heiri, O., Lotter, A.F., 2003. 9000 years of chironomid assemblage dynamics in an Alpine lake: long-term trends, sensitivity to disturbance, and resilience of the fauna. J. Paleolimnol. 30, 273–289.

Heiri, O., Lotter, A.F., 2010. How does taxonomic resolution affect chironomid-based temperature reconstruction? J. Paleolimnol. 44 (2), 589–601. https://doi.org/10.1007/s10933-010-9439-z.

Heiri, O., Lotter, A.F., Lemcke, G., 2001. Loss on ignition as a method for estimating organic and carbonate content in sediments: reproducibility and comparability of results. J. Paleolimnol. 25, 101–110.

Hughes, A.L.C., Gyllencreutz, R., Lohne, Ø.S., Mangerud, J., Svendsen, J.I., 2016. The last Eurasian ice sheets - a chronological database and time-slice reconstruction, DATED-1. Boreas 45 (1), 1–45. https://doi.org/10.1111/bor.12142.

Il'yashuk, B.P., Il'yashuk, E.A., 2000. Paleoecological analysis of chironomid assemblages of a mountain lake as a source of information for biomonitoring. Russ. J. Ecol. 31 (5), 353–358. https://doi.org/10.1007/BF02828451.

Il'yashuk, E.A., Il'yashuk, B.P., Hammarlund, D., Larocque, I., 2005. Holocene climatic and environmental changes inferred from midge records (Diptera: chironomidae, Chaoboridae, Ceratopogonidae) at Lake Berkut, southern Kola Peninsula, Russia. Holocene 15 (6), 897–914. https://doi.org/10.1191/0959683605hl865ra.

Il'yashuk, E.A., Il'yashuk, B.P., Kolka, V.V., Hammarlund, D., 2013. Holocene climate variability on the Kola Peninsula, Russian Subarctic, based on aquatic invertebrate records from lake sediments. Quaternary Research (United States) 79 (3), 350–361. https://doi.org/10.1016/j.yqres.2013.03.005.

IPCC, 2018. Global Warming of 1.5°C.An IPCC Special Report on the impacts of global warming of 1.5°C above pre-industrial levels and related global greenhouse gas emission pathways. In: Masson-Delmotte, V., Zhai, P., Pörtner, H.-O., Roberts, D., Skea, J., Shukla, P.R., Pirani, A., Moufouma-Okia, W., Péan, C., Pidcock, R., Connors, S., Matthews, J.B.R., Chen, Y., Zhou, X., Gomis, M.I., Lonnoy, E., Maycock, T., Tignor, M., Waterfield, T. (Eds.), The Context of Strengthening the Global Response to the Threat of Climate Change, Sustainable Development, and Efforts to Eradicate Poverty. Cambridge University Press. https://doi.org/10.1017/9781009157940. Cambridge, UK and New York, NY, USA, 616.

Jensen, C., Kuiper, J.G.J., Vorren, K.D., 2002. First post-glacial establishment of forest trees: early Holocene vegetation, mollusc settlement and climate dynamics in central Troms, North Norway. Boreas 31 (3), 285–301. https://doi.org/10.1111/j.1502-3885.2002.tb01074.x.

Juggins, S., 2015. Rioja: analysis of quaternary science data. R package. URL Http://Cran. r-Project. Org/Package= Rioja.

Juggins, S., Birks, H.J.B., 2012. Quantitative environmental reconstructions from biological data. In: Birks, H., Lotter, A., Juggins, S., Smol, J. (Eds.), Tracking Environmental Change Using Lake Sediments, Developments in Paleoenvironmental Research, vol. 5. Springer, Dordrecht. https://doi.org/10.1007/978-94-007-2745-8_14.

Karger, D.N., Conrad, O., Böhner, J., Kawohl, T., Kreft, H., Soria-Auza, R.W., Zimmermann, N.E., Linder, H.P., Kessler, M., 2017. Climatologies at high resolution for the earth's land surface areas. Sci. Data 4 (1), 1–20. https://doi.org/10.1038/sdata.2017.122.

Karger, D.N., Nobis, M.P., Normand, S., Graham, C.H., Zimmermann, N.E., 2023. CHELSA-TraCE21k - high-resolution (1 km) downscaled transient temperature and precipitation data since the Last Glacial Maximum. Clim. Past 19 (2), 439–456. https://doi.org/10.5194/cp-19-439-2023.

Korhola, A., Vasko, K., Toivonen, H.T.T., Olander, H., 2002. Holocene temperature changes in northern Fennoscandia reconstructed from chironomids using Bayesian modelling. Quat. Sci. Rev. 21 (16–17), 1841–1860. https://doi.org/10.1016/S0277-3791(02)00003-3.

Körner, C., 1998. A re-assessment of high elevation treeline positions and their explanation. Oecologia 115, 445–459. https://doi.org/10.1007/s004420050540.

Körner, C., 2018. Concepts in empirical plant ecology. Plant Ecol. Divers. 11 (4), 405–428. https://doi.org/10.1080/17550874.2018.1540021.

Langdon, P.G., Ruiz, Z., Brodersen, K.P., Foster, I.D.L., 2006. Assessing lake eutrophication using chironomids: understanding the nature of community response in different lake types. Freshw. Biol. 51 (3), 562–577. https://doi.org/10.1111/j.1365-2427.2005.01500.x.

Langdon, P.G., Ruiz, Z., Wynne, S., Sayer, C.D., Davidson, T.A., 2010. Ecological influences on larval chironomid communities in shallow lakes: implications for

palaeolimnological interpretations. Freshw. Biol. 55 (3), 531–545. https://doi.org/10.1111/j.1365-2427.2009.02345.x.
Leigh, J.R., Stokes, C.R., Evans, D.J.A., Carr, R.J., Andreassen, L.M., 2020. Timing of Little Ice Age maxima and subsequent glacier retreat in northern Troms and western Finnmark, northern Norway. Arctic Antarct. Alpine Res. 52 (1), 281–311. https://doi.org/10.1080/15230430.2020.1765520.
Lid, J., Lid, D., 2005. In: Elven, R.E. (Ed.), Norsk Flora, seventh ed., Det Norske Samlaget, p. 1230 Oslo.
Lim, D.S.S., Douglas, M.S.V., Smol, J.P., 2005. Limnology of 46 lakes and ponds on banks island, N.W.T., Canadian arctic archipelago. Hydrobiologia 545 (1), 11–32. https://doi.org/10.1007/s10750-005-1824-7.
Liu, M., Prentice, I.C., Ter Braak, C.J.F., Harrison, S.P., 2020. An improved statistical approach for reconstructing past climates from biotic assemblages: improved palaeoclimate reconstruction. Proc. R. Soc. A 476 (2243), 20200346. https://doi.org/10.1098/rspa.2020.0346.
Luoto, T.P., 2011. Indicator value of midge larvae (Diptera: nematocera) in shallow boreal lakes with a focus on habitat, water quality, and climate. Aquat. Insects 33 (4), 351–370. https://doi.org/10.1080/01650424.2011.640333.
Luoto, T.P., Kaukolehto, M., Nevalainen, L., 2014a. The relationship between water and air temperature in chironomid-based paleoclimate reconstructions: records from boreal and subarctic Finland. Holocene 24 (11), 1584–1590. https://doi.org/10.1177/0959683614544056.
Luoto, T.P., Kaukolehto, M., Weckström, J., Korhola, A., Väliranta, M., 2014b. New evidence of warm early-Holocene summers in subarctic Finland based on an enhanced regional chironomid-based temperature calibration model. Quaternary Research 81 (1), 50–62. https://doi.org/10.1016/j.yqres.2013.09.010.
Luoto, T.P., Salonen, V.P., 2010. Fossil midge larvae (Diptera: chironomidae) as quantitative indicators of late-winter hypolimnetic oxygen in southern Finland: a calibration model, case studies and potentialities. Boreal Environ. Res. 15 (1), 1–18, 1.
MacDonald, G.M., Edwards, T.W.D., Moser, K.A., Pienitz, R., Smol, J.P., 1993. Rapid response of treeline vegetation and lakes to past climate warming. Nature 361 (6409), 243–246. https://doi.org/10.1038/361243a0.
Macias-Fauria, M., Forbes, B.C., Zetterberg, P., Kumpula, T., 2012. Eurasian Arctic greening reveals teleconnections and the potential for structurally novel ecosystems. Nat. Clim. Change 2 (8), 613–618. https://doi.org/10.1038/nclimate1558.
Mann, D.H., Peteet, D.M., Reanier, R.E., Kunz, M.L., 2002. Responses of an arctic landscape to Lateglacial and early Holocene climatic changes: the importance of moisture. Quat. Sci. Rev. 21 (8–9), 997–1021. https://doi.org/10.1016/S0277-3791(01)00116-0.
Mann, M.E., Zhang, Z., Rutherford, S., Bradley, R.S., Hughes, M.K., Shindell, D., Ammann, C., Faluvegi, G., Ni, F., 2009. Global signatures and dynamical origins of the little ice age and medieval climate anomaly. Science 326 (5957), 997–1021. https://doi.org/10.1126/science.1177303.
Mayfield, R.J., Langdon, P.G., Doncaster, C.P., Dearing, J.A., Wang, R., Velle, G., Davies, K.L., Brooks, S.J., 2021. Late Quaternary chironomid community structure shaped by rate and magnitude of climate change. J. Quat. Sci. 36 (3), 360–376. https://doi.org/10.1002/jqs.3301.
McGowan, S., Anderson, N.J., Edwards, M.E., Hopla, E., Jones, V., Langdon, P.G., Law, A., Solovieva, N., Turner, S., van Hardenbroek, M., Whiteford, E.J., Wiik, E., 2018. Vegetation transitions drive the autotrophy–heterotrophy balance in Arctic lakes. Limnology And Oceanography Letters 3 (3), 246–255. https://doi.org/10.1002/lol2.10086.
Medeiros, A.S., Biastoch, R.G., Luszczek, C.E., Wang, X.A., Muir, D.C.G., Quinlan, R., 2012. Patterns in the limnology of lakes and ponds across multiple local and regional environmental gradients in the eastern canadian arctic. Inland Waters 2 (2), 59–76. https://doi.org/10.5268/IW-2.2.427.
Medeiros, A.S., Milošević, Đ., Francis, D.R., Maddison, E., Woodroffe, S., Long, A., Walker, I.R., Hamerlík, L., Quinlan, R., Langdon, P., Brodersen, K.P., Axford, Y., 2021. Arctic chironomids of the northwest North Atlantic reflect environmental and biogeographic gradients. J. Biogeogr. 48 (3), 511–525. https://doi.org/10.1111/jbi.14015.
Medeiros, A.S., Quinlan, R., 2011. The distribution of the Chironomidae (Insecta: Diptera) along multiple environmental gradients in lakes and ponds of the eastern Canadian Arctic. Can. J. Fish. Aquat. Sci. 68 (9), 1511–1527. https://doi.org/10.1139/f2011-076.
Mekonnen, Z.A., Riley, W.J., Berner, L.T., Bouskill, N.J., Torn, M.S., Iwahana, G., Breen, A.L., Myers-Smith, I.H., Criado, M.G., Liu, Y., Euskirchen, E.S., Goetz, S.J., Mack, M.C., Grant, R.F., 2021. Arctic tundra shrubification: a review of mechanisms and impacts on ecosystem carbon balance. Environ. Res. Lett. 16 (5), 053001. https://doi.org/10.1088/1748-9326/abf28b.
Miller, P.A., Giesecke, T., Hickler, T., Bradshaw, R.H.W., Smith, B., Seppä, H., Valdes, P. J., Sykes, M.T., 2008. Exploring climatic and biotic controls on Holocene vegetation change in Fennoscandia. J. Ecol. 96 (2), 247–259. https://doi.org/10.1111/j.1365-2745.2007.01342.x.
Mjelde, M., Thrane, J.E., Demars, B.O.L., 2023. High aquatic macrophyte diversity in Norwegian lakes north of the Arctic Circle. Freshw. Biol. 68 (3), 509–522. https://doi.org/10.1111/fwb.14043.
Mörner, N.A., 2003. Paleoseismicity of Sweden. *A Novel Paradigm*. JOFO Grafiska AB. Stockholm. ISBN–91–631-4072-1.
Nazarova, L., Bleibtreu, A., Hoff, U., Dirksen, V., Diekmann, B., 2017. Changes in temperature and water depth of a small mountain lake during the past 3000 years in Central Kamchatka reflected by a chironomid record. Quat. Int. 447, 46–58. https://doi.org/10.1016/j.quaint.2016.10.008.
Nesje, A., 1992. A piston corer for lacustrine and marine sediments. Arct. Alp. Res. 24 (3), 257–259. https://doi.org/10.1080/00040851.1992.12002956.
Nesje, A., 2009. Latest pleistocene and Holocene alpine glacier fluctuations in scandinavia. Quat. Sci. Rev. 28 (21–22), 2119–2213. https://doi.org/10.1016/j.quascirev.2008.12.016.
NGU, 2023. Norges Geologiske Undersøkelse (NGU), Geological Maps of Norway.
Nolan, C., Overpeck, J.T., Allen, J.R.M., Anderson, P.M., Betancourt, J.L., Binney, H.A., Brewer, S., Bush, M.B., Chase, B.M., Cheddadi, R., Djamali, M., Dodson, J., Edwards, M.E., Gosling, W.D., Haberle, S., Hotchkiss, S.C., Huntley, B., Ivory, S.J., Kershaw, A.P., et al., 2018. Past and future global transformation of terrestrial ecosystems under climate change. Science 361 (6405), 920–923. https://doi.org/10.1126/science.aan5360.
Oksanen, J., Blanchet, F.G., Friendly, M., Kindt, R., Legendre, P., Wagner, H., 2020. Vegan: community ecology package version 2.5-7. https://cran.r-project.org/web/packages/vegan/index.html.
Olander, H., Birks, H.J.B., Korhola, A., Blom, T., 1999. An expanded calibration model for inferring lakewater and air temperatures from fossil chironomid assemblages in northern Fennoscandia. Holocene 9 (3), 279–294.
Otiniano, G.A., Porter, T.J., Phillips, M.A., Juutinen, S., Weckström, J.B., Heikkilä, M.P., 2024. Reconstructing warm-season temperatures using brGDGTs and assessing biases in Holocene temperature records in northern Fennoscandia. Quat. Sci. Rev. 329, 108555. https://doi.org/10.1016/j.quascirev.2024.108555.
Pasvik National Nature Reserve, 2023. Pasvik National Nature Reserve en.pasvik-reserve.ru/climate. (Accessed 1 April 2023).
Pearson, R.G., Phillips, S.J., Loranty, M.M., Beck, P.S.A., Damoulas, T., Knight, S.J., Goetz, S.J., 2013. Shifts in Arctic vegetation and associated feedbacks under climate change. Nat. Clim. Change 3 (7), 673–677. https://doi.org/10.1038/nclimate1858.
Perret-Gentil, N., Rey, F., Gobet, E., Tinner, W., Heiri, O., 2024. Human impact leads to unexpected oligotrophication and deepwater oxygen increase in a Swiss mountain lake. Holocene 34 (2), 189–201. https://doi.org/10.1177/09596836231211821.
Pinder, L., 1983. The larvae of Chironominae (Diptera: chironomidae) of the Holarctic region-Keys and diagnoses. Chironomidae of the Holarctic Region. Keys and Diagnoses, 1. Larvae, Entomol. Scand. Suppl. 19, 149–294.
Porinchu, D.F., Cwynar, L.C., 2000. The distribution of freshwater chironomidae (insecto: Diptera) across treeline near the lower lena river, northeast siberia, Russia. Arctic Antarct. Alpine Res. 32 (4), 429–437. https://doi.org/10.2307/1552392.
Post, E., Alley, R.B., Christensen, T.R., Macias-Fauria, M., Forbes, B.C., Gooseff, M.N., Iler, A., Kerby, J.T., Laidre, K.L., Mann, M.E., Olofsson, J., Stroeve, J.C., Ulmer, F., Virginia, R.A., Wang, M., 2019. The polar regions in a 2°C warmer world. Sci. Adv. 5 (12), eaaw9883. https://doi.org/10.1126/sciadv.aaw9883.
Quinlan, R., Smol, J.P., 2001. Chironomid-based inference models for estimating end-of-summer hypolimnetic oxygen from south-central Ontario shield lakes. Freshw. Biol. 46 (11), 1529–1551.
R Core Team, 2019. R: A Language and Environment for Statistical Computing. R-project.org/.
Ranta, H., Kubin, E., Siljamo, P., Sofiev, M., Linkosalo, T., Oksanen, A., Bondestam, K., 2006. Long distance pollen transport cause problems for determining the timing of birch pollen season in Fennoscandia by using phenological observations. Grana 45 (4), 297–304. https://doi.org/10.1080/00173130600984740.
Räsänen, S., 2001. Tracing and interpreting fine-scale human impact in Northern Fennoscandia with the aid of modern pollen analogues. Veg. Hist. Archaeobotany 10 (4), 211–218. https://doi.org/10.1007/PL00006932.
Rasmussen, S.O., Vinther, B.M., Clausen, H.B., Andersen, K.K., 2007. Early Holocene climate oscillations recorded in three Greenland ice cores. Quat. Sci. Rev. 26 (15–16), 1907–1914. https://doi.org/10.1016/j.quascirev.2007.06.015.
Reimer, P.J., Austin, W.E.N., Bard, E., Bayliss, A., Blackwell, P.G., Bronk Ramsey, C., Butzin, M., Cheng, H., Edwards, R.L., Friedrich, M., Grootes, P.M., Guilderson, T.P., Hajdas, I., Heaton, T.J., Hogg, A.G., Hughen, K.A., Kromer, B., Manning, S.W., Muscheler, R., et al., 2020. The IntCal20 northern hemisphere radiocarbon age calibration curve (0-55 cal kBP). Radiocarbon 62 (4), 725–757. https://doi.org/10.1017/RDC.2020.41.
Renberg, I., Battarbee, R.W., Mason, B.J., Renberg, 1, Talling, J.F., 1990. A 12600 year perspective of the acidification of Lilia Oresjon, southwest Sweden. Philosophical Transactions of the Royal Society B 327, 357–361.
Revéret, A., Rijal, D.P., Heintzman, P.D., Brown, A.G., Stoof-Leichsenring, K.R., Alsos, I. G., 2023. Environmental DNA of aquatic macrophytes: the potential for reconstructing past and present vegetation and environments. Freshw. Biol. 68 (11), 1929–1950. https://doi.org/10.1111/fwb.14158.
Rijal, D.P., Heintzman, P.D., Lammers, Y., Yoccoz, N.G., Lorberau, K.E., Pitelkova, I., Goslar, T., Murguzur, F.J.A., Salonen, J.S., Helmens, K.F., Bakke, J., Edwards, M.E., Alm, T., Bråthen, K.A., Brown, A.G., Alsos, I.G., 2021. Sedimentary ancient DNA shows terrestrial plant richness continuously increased over the Holocene in northern Fennoscandia. Sci. Adv. 7 (31), eabf9557. https://doi.org/10.1126/sciadv.abf9557.
Romundset, A., Bondevik, S., Bennike, O., 2011. Postglacial uplift and relative sea level changes in Finnmark, northern Norway. Quat. Sci. Rev. 30 (19–20), 2398–2421. https://doi.org/10.1016/j.quascirev.2011.06.007.
Rørslett, B., 1991. Principal determinants of aquatic macrophyte richness in northern European lakes. Aquat. Bot. 39 (1–2), 173–193. https://doi.org/10.1016/0304-3770(91)90031-Y.
Salonen, J.S., Kuosmanen, N., Alsos, I.G., Heintzman, P.D., Rijal, D.P., Schenk, F., Bogren, F., Luoto, M., Philip, A., Piilo, S., Trasune, L., Väliranta, M., Helmens, K.F., 2024. Uncovering Holocene climate fluctuations and ancient conifer populations: insights from a high-resolution multi-proxy record from Northern Finland. Global Planet. Change 237, 104462. https://doi.org/10.1016/j.gloplacha.2024.104462.
Sarmaja-Korjonen, K., Nyman, M., Kultti, S., Väliranta, M., 2006. Palaeolimnological development of Lake Njargajavri, northern Finnish Lapland, in a changing Holocene

climate and environment. J. Paleolimnol. 35 (1), 65–81. https://doi.org/10.1007/s10933-005-7337-6.
Sejrup, H.P., Seppä, H., McKay, N.P., Kaufman, D.S., Geirsdóttir, Á., de Vernal, A., Renssen, H., Husum, K., Jennings, A., Andrews, J.T., 2016. North Atlantic-Fennoscandian Holocene climate trends and mechanisms. Quat. Sci. Rev. 147, 365–378. https://doi.org/10.1016/j.quascirev.2016.06.005.
Seppä, H., 1998. Postglacial trends in palynological richness in the northern Fennoscandian tree-line area and their ecological interpretation. Holocene 8 (1), 43–53. https://doi.org/10.1191/095968398674096317.
Seppä, H., & Birks, H. J. B. (2001). July mean temperature and annual precipitation trends during the Holocene in the Fennoscandian tree-line area: Pollen-based climate reconstructions. Holocene, 11(5), pp.527-539. https://doi.org/10.1191/095968301680223486.
Seppä, H., Birks, H.J.B., Odland, A., Poska, A., Veski, S., 2004. A modern pollen-climate calibration set from northern Europe: developing and testing a tool for palaeoclimatological reconstructions. J. Biogeogr. 31 (2), 251–267. https://doi.org/10.1111/j.1365-2699.2004.00923.x.
Seppä, H., Nyman, M., Korhola, A., Weckström, J., 2002. Changes of treelines and alpine vegetation in relation to post-glacial climate dynamics in northern Fennoscandia based on pollen and chironomid records. J. Quat. Sci. 17 (4), 287–301. https://doi.org/10.1002/jqs.678.
Serafin, A., Pogorzelec, M., Bronowicka-Mielniczuk, U., 2017. The specificity of natural habitats of menyanthes trifoliata L. In peat bogs of the central part of eastern Poland. Appl. Ecol. Environ. Res. 15 (3), 849–859. https://doi.org/10.15666/aeer/1503_849859.
Shala, S., Helmens, K.F., Luoto, T.P., Salonen, J.S., Väliranta, M., Weckström, J., 2017. Comparison of quantitative Holocene temperature reconstructions using multiple proxies from a northern boreal lake. Holocene 27 (11), 1745–1755. https://doi.org/10.1177/0959683617708442.
Simpson, G.L., Oksanen, J., 2019. analogue: Analogue matching and Modern Analogue Technique transfer function models. (R package version 0.17-3).
Sjögren, P., Damm, C., 2019. Holocene vegetation change in northernmost Fennoscandia and the impact on prehistoric foragers 12 000–2000 cal. a BP – a review. Boreas 48 (1), 20–35. https://doi.org/10.1111/bor.12344.
Skandfer, M., Høeg, H.I., 2012. Bácheveaij/Pasvikdalens Eldre Historie Belyst Ved Pollenanalyser Og Arkeologisk Materiale. Viking. Norsk Arkeologisk Selskap. Available at: Https://Munin.Uit.No/Handle/10037/4788 (Accessed 14 January 2023).
Smith, S.J., Edmonds, J., Hartin, C.A., Mundra, A., Calvin, K., 2015. Near-term acceleration in the rate of temperature change. Nat. Clim. Change 5 (4), 333–336. https://doi.org/10.1038/nclimate2552.
Staehr, P.A., Baastrup-Spohr, L., Sand-Jensen, K., Stedmon, C., 2012. Lake metabolism scales with lake morphometry and catchment conditions. Aquat. Sci. 74 (1), 155–169. https://doi.org/10.1007/s00027-011-0207-6.
Taberlet, P., Coissac, E., Pompanon, F., Brochmann, C., Willerslev, E., 2012. Towards next-generation biodiversity assessment using DNA metabarcoding. Mol. Ecol. 21 (8), 2045–2050.
Telford, R.J., 2015. palaeoSig: significance Tests of quantitative palaeoenvironmental reconstructions. R package version (1), 1–3 cran.nexr.com/web/packages/palaeoSig/citation.html. (Accessed 14 January 2023).
Telford, R.J., Birks, H.J.B., 2011. A novel method for assessing the statistical significance of quantitative reconstructions inferred from biotic assemblages. Quat. Sci. Rev. 30 (9–10), 1272–1278. https://doi.org/10.1016/j.quascirev.2011.03.002.
Ter Braak, C.J.F., Juggins, S., 1993. Weighted averaging partial least squares regression (WA-PLS): an improved method for reconstructing environmental variables from species assemblages. Hydrobiologia 269, 485–502. https://doi.org/10.1007/978-94-017-3622-0_49.
Ter Braak, C.J.F., Juggins, S., Birks, H.J.B., Van Der Voet, H., 1993. Weighted Averaging Partial Least Squares regression (WA-PLS): definition and comparison with other methods for species-environment calibration. Multivariate environmental statistics (6), 525–560. Available at: https://edepot.wur.nl/249353.
Tiwari, T., Sponseller, R.A., Laudon, H., 2018. Extreme climate effects on dissolved organic carbon concentrations during snowmelt. J. Geophys. Res.: Biogeosciences 123 (4), 1277–1288. https://doi.org/10.1002/2017JG004272.
Tyler, T., Herbertsson, L., Olofsson, J., Olsson, P.A., 2021. Ecological indicator and traits values for Swedish vascular plants. Ecol. Indicat. 120, 106923. https://doi.org/10.1016/j.ecolind.2020.106923.
Ursenbacher, S., Stötter, T., Heiri, O., 2020. Chitinous aquatic invertebrate assemblages in Quaternary lake sediments as indicators of past deepwater oxygen concentration. Quat. Sci. Rev. 231, 10620. https://doi.org/10.1016/j.quascirev.2020.106203.
Väliranta, M., Salonen, J.S., Heikkilä, M., Amon, L., Helmens, K., Klimaschewski, A., Kuhry, P., Kultti, S., Poska, A., Shala, S., Veski, S., Birks, H.H., 2015. Plant macrofossil evidence for an early onset of the Holocene summer thermal maximum in northernmost Europe. Nat. Commun. 6 (1), 6809. https://doi.org/10.1038/ncomms7809.
Velle, G., Brodersen, K.P., Birks, H.J.B., Willassen, E., 2010. Midges as quantitative temperature indicator species: lessons for palaeoecology. Holocene 20 (6), 989–1002. https://doi.org/10.1177/0959683610365933.
Velle, G., Brooks, S.J., Birks, H.J.B., Willassen, E., 2005. Chironomids as a tool for inferring Holocene climate: an assessment based on six sites in southern Scandinavia. Quat. Sci. Rev. 24 (12–13), 1429–1462. https://doi.org/10.1016/j.quascirev.2004.10.010.
Wagner, N.D., Volf, M., Hörandl, E., 2021. Highly diverse shrub willows (Salix L.) share highly similar plastomes. Front. Plant Sci. 12, 662715. https://doi.org/10.3389/fpls.2021.662715.
Walsh, J.E., Fetterer, F., Stewart, J.S., Chapman, W.L., 2016. A database for depicting Arctic sea ice variations back to 1850. Geographical Review 107 (1), 89–107. https://doi.org/10.1111/j.1931-0846.2016.12195.x.
Wanner, H., Beer, J., Bütikofer, J., Crowley, T.J., Cubasch, U., Flückiger, J., Goosse, H., Grosjean, M., Joos, F., Kaplan, J.O., Küttel, M., Müller, S.A., Prentice, I.C., Solomina, O., Stocker, T.F., Tarasov, P., Wagner, M., Widmann, M., 2008. Mid- to Late Holocene climate change: an overview. Quat. Sci. Rev. 27 (19–20), 1791–1828. https://doi.org/10.1016/j.quascirev.2008.06.013.
Wiederholm, T., Eriksson, L., 1977. Benthos of an acid lake. Oikos 29, 261–267.
Wolff, E.W., Chappellaz, J., Blunier, T., Rasmussen, S.O., Svensson, A., 2010. Millennial-scale variability during the last glacial: the ice core record. Quat. Sci. Rev. 29 (21–22), 2828–2838. https://doi.org/10.1016/j.quascirev.2009.10.013.
Zellweger, F., Sulmoni, E., Malle, J.T., Baltensweiler, A., Jonas, T., Zimmermann, N.E., Ginzler, C., Karger, D.N., De Frenne, P., Frey, D., Webster, C., 2024. Microclimate mapping using novel radiative transfer modelling. Biogeosciences 21 (2), 605–623. https://doi.org/10.5194/bg-21-605-2024.